Copy No. [redacted]

RM No. L8J01

[redacted]

NACA RM No. L8J01

RM L8J01

7151

TECH LIBRARY KAFB, NM

0143874

NACA

RESEARCH MEMORANDUM

INVESTIGATION OF HORN BALANCES ON A 45° SWEPTBACK HORIZONTAL TAIL SURFACE AT HIGH SUBSONIC SPEEDS

By

Harold S. Johnson and Robert F. Thompson

Langley Aeronautical Laboratory
Langley Field, Va.

CLASSIFIED DOCUMENT

[redacted]

NATIONAL ADVISORY COMMITTEE
FOR AERONAUTICS

WASHINGTON

December 3, 1948

[redacted]

Classification cancelled (or changed to Unclassified

By Authority of NASA Tech Pub Announcement

(OFFICER AUTHORIZED TO CHANGE)

37 29 Jan 64

By

NK

GRADE OF OFFICER MAKING CHANGE)

11 April

DATE

TECH LIBRARY KAFB, NM
0143874

NATIONAL ADVISORY COMMITTEE FOR AERONAUTICS

RESEARCH MEMORANDUM

INVESTIGATION OF HORN BALANCES ON A 45° SWEPTBACK HORIZONTAL TAIL SURFACE AT HIGH SUBSONIC SPEEDS

By Harold S. Johnson and Robert F. Thompson

SUMMARY

An investigation was made in the Langley 300 mph and high-speed 7- by 10-foot tunnels of the aerodynamic characteristics of a 45° swept-back, semispan, horizontal tail surface equipped with a horn-balanced 25-percent-chord elevator. The effects of horn size and horn inboard-edge fairing were determined at low speed and one of the configurations was investigated through a speed range to a Mach number of 0.89.

The studies at low speed showed that the horn was effective on a swept horizontal tail and that a given change in horn size was about five times as effective in balancing the variation of hinge moment with deflection C_{h_δ} as the change of hinge moment with angle of attack C_{h_α}. Fairing the horn inboard edge reduced the effectiveness of horn in balancing the hinge moments caused by elevator deflection.

Although the particular arrangement investigated through the speed range was overbalanced at moderate and high speeds, it is believed that modifications such as a decrease in horn-balance size or a reduction in elevator trailing-edge angle may make the horn type of balance satisfactory up to high subsonic speeds.

The change in lift coefficient with elevator deflection C_{L_δ} increased slightly as the horn size became larger and was unaffected by changes in Mach number for the speed range investigated.

INTRODUCTION

The necessity of providing a means of reducing the high-speed control forces of the faster, more heavily loaded airplanes currently in use or being designed while retaining sufficient control for landing and take-off has presented a problem to airplane designers. Even though a control

system incorporates a power boost, it is desirable to balance aerodynamically as much of the control force as possible. It has been found that the use of a horn balance is one method of reducing the aerodynamic hinge moments at low speeds (references 1 to 4). In addition, the horn type of balance provides a convenient attachment for counterbalances to statically balance the control. In order to provide additional information on the characteristics of balanced control surfaces suitable for high subsonic speeds, an investigation is being conducted in the Langley 7- by 10-foot tunnels. This report presents the results of an investigation of a 45° sweptback, untapered, semispan, horizontal-tail model equipped with a horn-balanced elevator.

In order to determine the effects of horn size and of fairing the horn inboard edge (normal to hinge axis) on the hinge-moment parameters, three sizes of horns were investigated at a low Mach number ($M = 0.30$). One of these configurations that appeared satisfactory at low speed was investigated through a speed range up to a Mach number of 0.89. The effects of fixing transition were also studied at several Mach numbers.

MODEL AND APPARATUS

The semispan horizontal-tail model used for the investigation had an NACA 0012 airfoil section perpendicular to the leading edge, an aspect ratio of 3.00 (based on the full-span dimensions), a taper ratio of 1, 45° of sweepback, and was equipped with a 0.25c' unsealed, horn-balanced elevator with a radius elevator nose. The model was constructed of hardened steel to the plan form indicated in figure 1. The radius tip and the horn filler blocks were constructed of wood. The horn balance was triangular in shape and the horn inboard edge was perpendicular to the elevator hinge axis. The model was so constructed that the size of the horn could be changed by attaching filler blocks to the inboard edge of the horn or to the wing. Three amounts of balance (table I), referred to in the text and on the figures as the small, intermediate, and large horn, were tested; in addition, the intermediate horn was tested with a rounded inboard edge, referred to herein as the faired horn. The dimensional characteristics of the four horns are presented in figure 2 and table I. Structural calculations indicated that more than two hinges would be necessary. Reference 5 indicates that for elevators having three hinges the hinge-moment increments resulting from distortion can be an appreciable fraction of the total hinge moment. To avoid the inclusion of these structural hinge-moment increments, the elevator was constructed in two spanwise segments and the $\frac{1}{16}$-inch gap between the two halves was unsealed. The elevator hinge moments were measured by calibrated beam-type electrical strain gages mounted within the stabilizer. The elevator deflections were varied by changing the strain-gage yokes attached to the elevator.

[redacted]

E R R A T U M

NACA RM L8J01

INVESTIGATION OF HORN BALANCES ON A 45° SWEPTBACK HORIZONTAL TAIL SURFACE AT HIGH SUBSONIC SPEEDS

By Harold S. Johnson and Robert F. Thompson

December 3, 1948

Page 3: The formula following the definition of the coefficient C_h is in error and the symbol b therein should be replaced with the symbol b_1, which is defined as "twice the elevator semispan measured along hinge line, feet."

[redacted]

NACA-Langley - 1-30-50 - 425

[redacted]

The semispan model was mounted vertically in the Langley 300 mph and high-speed 7- by 10-foot tunnels as shown in figure 3 with the root chord adjacent to the tunnel ceiling which thereby acted as a reflection plane. The model was supported entirely by the balance frame so that all forces and moments acting on the model could be measured. A small clearence was maintained between the model and the tunnel ceiling. A metal end plate was attached to the model to deflect the air flowing into the test section through the clearance hole in order to minimize the effect of this air flow on the flow over the model. Provisions were made for changing the angle of attack of the model while the tunnel was in operation.

Most of the tests were performed with transition free on the model. For the tests with transition fixed, 0.008-inch-diameter carborundum grains were sparsely spread over both the upper and lower surfaces of the model at the 10-percent-chord station in $\frac{3}{8}$-inch-wide strips.

The Langley 300 mph and high-speed 7- by 10-foot tunnels are closed-throat, single-return tunnels. Turbulence measurements made in the 300 mph tunnel indicated that the turbulence factor is very close to unity. Though the turbulence of the high-speed-tunnel air stream has not been determined, it is also thought to be low since both tunnels have large tunnel-contraction ratios (about 14 to 1).

COEFFICIENTS AND SYMBOLS

The coefficients and symbols used in this paper are defined as follows:

C_L lift coefficient (L/qS)

C_D drag coefficient (D/qS)

C_m pitching-moment coefficient (M/qSc')

C_h elevator hinge-moment coefficient $\left(H/q\left(\right)\bar{c}_e^{\,2}\right)$ see erratum.

L twice lift of semispan model, pounds

D twice drag of semispan model, pounds

M twice pitching moment of semispan model, measured about the low-speed aerodynamic center (1.63 ft behind root-chord leading edge), foot-pounds

[redacted]

H twice hinge moment of semispan model elevator measured about the elevator hinge line, foot-pounds

S twice area of semispan model, 9.21 square feet

S_e area of semispan model elevator behind hinge line, 1.15 square feet

S_H area of model horn, square feet (See table I.)

b twice span of semispan model, 5.26 feet

c' mean aerodynamic chord, 1.77 feet

$\bar{c}_e$ root-mean-square chord of model elevator behind hinge line (measured perpendicular to hinge line), 0.31 foot

c_e average chord of model elevator behind hinge line (measured perpendicular to hinge line), 0.31 foot

c_H average chord of model horn (measured perpendicular to hinge line), feet (See table I.)

B balance coefficient $\left(\sqrt{S_H c_H / S_e c_e}\right)$

α angle of attack of model with respect to chord plane, degrees

δ_e elevator deflection relative to stabilizer, measured normal to the elevator hinge line (positive when trailing edge is down), degrees

M Mach number (V/a)

V free-stream velocity, feet per second

q free-stream dynamic pressure, pounds per square foot $\left(\frac{1}{2}\rho V^2\right)$

ρ mass density of air, slugs per cubic foot

a speed of sound, feet per second

$C_{h_\alpha} = \left(\frac{\partial C_h}{\partial \alpha}\right)_{\delta_e}$

$$C_{h_\delta} = \left(\frac{\partial C_h}{\partial \delta_e}\right)_\alpha$$

$$C_{L_\alpha} = \left(\frac{\partial C_L}{\partial \alpha}\right)_{\delta_e}$$

$$C_{L_\delta} = \left(\frac{\partial C_L}{\partial \delta_e}\right)_\alpha$$

$$\alpha_\delta = \left(\frac{C_{L_\delta}}{C_{L_\alpha}}\right)$$

The subscripts outside the parentheses indicate the factors held constant during the measurement of the parameters. The slopes were measured in the vicinity of $\alpha = 0^\circ$ and $\delta_e = 0^\circ$.

CORRECTIONS

Jet-boundary corrections were applied to the angles of attack and to the drag-coefficient data in accordance with the following equations which were determined by the method of reference 6, using unpublished values of boundary-induced upwash computed for swept wings:

$$\alpha = \alpha_M + 0.553\ C_{L_M}$$

$$C_D = C_{D_M} + 0.0083\ C_{L_M}{}^2$$

where the subscript M indicates measured values. The jet-boundary corrections to the lift, pitching-moment, and hinge-moment data were considered negligible and hence were not applied.

All coefficients and Mach numbers were corrected for blocking by the model and its wake. The blockage corrections were computed by the methods presented in reference 7.

The deflection of the model under load is believed to have been small, and, therefore, to have a negligible effect on the aerodynamic characteristics of the model. Corrections to the elevator angle due to deflection under load, though of small magnitude, have been applied at $\alpha = 0^{\circ}$. No attempt was made to correct for the air flow through the gap at the root of the model or between the two elevator segments.

TESTS AND TEST CONDITIONS

For the model equipped with the faired and the large horn balances, test data were obtained for ten values of elevator deflection covering a range of from 0° to -30°. For the model with the small and intermediate horns, the elevator deflection range was limited to -7.8°. The tests were made through an angle-of-attack range of from 0° through the positive stall and from 0° through the negative stall except for conditions where tunnel power limitations restricted the angle-of-attack range. The model with the faired horn was tested at eight values of Mach number covering a range of from 0.30 to 0.89. The tests of the model equipped with the small, intermediate, and large horns were made at $M = 0.30$ in the Langley 300 mph 7- by 10-foot tunnel. For clarity on the figures, not all of the test data are presented. All the test data were used in the determination of the various parameters.

Tests were made at several representative Mach numbers to determine the effects of fixing transition.

The choking Mach number of the high-speed tunnel, based on one-dimensional-flow theory and the dimensions of the present model, was estimated to be about 0.92. With this choking Mach number, experience has indicated that the data would be valid up to the highest Mach number (0.89) obtained during the tests.

The variation of test Reynolds number with Mach number for average test conditions is presented as figure 4. The Reynolds numbers are based on the mean aerodynamic chord (1.77 ft).

DISCUSSION

Effect of Horn Size

The variation of the aerodynamic coefficients C_L, C_D, C_m, and C_h with angle of attack at a Mach number of 0.30 is presented in figures 5 to 7 for the three sizes of horns tested. The hinge-moment coefficients presented are for the complete elevator, (the summation of the hinge moments of the two spanwise segments).

The effect of horn size on the hinge-moment parameters C_{h_α} and C_{h_δ} is shown in figure 8 and table II where the horn size is expressed by the term balance coefficient $B = \sqrt{S_H c_H / S_e c_e}$, which previous analyses have shown to be a good indication of balance effectiveness. (See references 2 to 4.) As expected, C_{h_α} and C_{h_δ} increased positively with increasing horn size. C_{h_δ} changed more rapidly than C_{h_α} for a given change in balance coefficient, the ratio being about five to one. This is much larger than for the horn balance on unswept surfaces where the ratio was more nearly one. The elevator was overbalanced for balance coefficients greater than about 0.31. The rate of change of hinge-moment coefficient with angle of attack became positive at a balance coefficient of about 0.38.

The effect of horn size on the lift parameters is shown in figure 9 and table II. As expected, the rate of change of lift coefficient with angle of attack C_{L_α} was relatively unaffected by changes in horn size. As the balance coefficient was increased, the rate of change of lift coefficient with elevator deflection C_{L_δ} and thereby the elevator-effectiveness parameter α_δ increased slightly. The numerical increases in C_{L_δ} and α_δ are attributed to the increased area of the elevator.

Effect of Horn Inboard-Edge Shape

Additional tests were made with the flat inboard edge of the intermediate horn faired (fig. 10). Fairing the inboard edge of the intermediate-size horn resulted in a large decrease in C_{h_δ} (from 0.0025 to -0.0014) and eliminated the overbalanced condition (fig. 8 and table II), but had little effect on C_{h_α}. Reference 4 shows a similar effect of horn nose

shape on the hinge-moment parameters for an unswept tail surface. These results indicate that the inboard edge of the present horn acts as a leading edge and that varying the horn nose shape provides the designer with a powerful tool for adjusting the balancing characteristics of a control surface once a satisfactory value of rate of change of hinge-moment coefficient with angle of attack is obtained.

The horn inboard-edge shape had little or no effect on the control-surface lift characteristics. (See fig. 9 and table II.)

To provide the small control forces and the control response desired, C_{h_δ} should have a small negative value and the value of C_{h_α} should be near zero. On this basis, the model with the faired horn leading edge exhibited the most desirable hinge-moment characteristics at low speeds.

Effect of Mach Number

The aerodynamic characteristics of the faired horn through the speed range up to $M = 0.89$ are presented as figures 11 to 18. The variation of the hinge-moment parameters C_{h_α} and C_{h_δ} with Mach number (fig. 19) shows that C_{h_δ} decreased negatively (or increased positively) with increasing Mach number, and the elevator was overbalanced at Mach numbers greater than about 0.63. The change in C_{h_δ} with Mach number is fairly linear up to a Mach number of about 0.80; for Mach numbers greater than 0.82, C_{h_δ} increased rapidly with Mach number. A study of the hinge-moment characteristics of the inboard and outboard portions of the elevator (data not presented) shows that the C_{h_δ} values for the inboard segment of the elevator did not vary with Mach number. Since the inboard portion of the elevator exhibited no variation of C_{h_δ} with Mach number and the effects of spanwise control-surface location on the hinge-moment parameters of unbalanced surfaces at low Mach numbers are small (reference 8), it is believed that most of the positive increase in C_{h_δ} with Mach number may be attributed to the fact that the balancing power of the horn becomes more effective at higher Mach numbers. The parameter C_{h_α} increased positively with Mach number, more rapidly at the higher Mach numbers, and attained a value of about 0.0016 at $M = 0.89$. In addition, a study of figures 11 to 18 reveals that both C_{h_α} and C_{h_δ} generally increased negatively as the angle of attack is varied from $\alpha = 0^\circ$.

Because of the overbalancing tendencies shown at high Mach numbers, the results indicate that the horn tested was too large. Decreasing the horn size would reduce or eliminate these overbalancing tendencies although the low-speed stick forces would be increased. These overbalancing tendencies at the higher Mach numbers would probably be eliminated by using a horn balance on a control surface having a small trailing-edge angle. (See reference 9.)

The variation of the lift parameters C_{L_α} and C_{L_δ} and the elevator-effectiveness factor α_δ with Mach number is shown in figure 20. These data show that C_{L_α} increased with Mach number, and that for the Mach number range tested the rate of increase of C_{L_α} with M was more rapid at the higher Mach numbers; the values of C_{L_α} increased from about 0.043 at $M = 0.30$ to 0.051 at $M = 0.89$. Also presented in figure 20 are values of C_{L_α} determined by the method of reference 10. Though the theoretical values are high, the variations of the lift-curve slopes with Mach number obtained experimentally and theoretically are in very good agreement. The theoretical values would be expected to be high since the method of reference 10 is based on a section lift-curve slope of 2π per radian.

The parameter C_{L_δ} did not vary with Mach number and had a value of 0.015 for the speed range investigated (fig. 20). However, at elevator deflection greater than -10°, the lift coefficient for a given deflection decreased with speed (fig. 21), the decrease becoming more marked as the elevator deflections were increased. This decrease in lift coefficient as M was increased for elevator deflections of greater than -10° is probably due to the fact that the critical speed of the tail surface is reached at lower values of Mach number with large elevator deflections.

Because of the aforementioned changes in C_{L_α} and C_{L_δ} with M, the elevator effectiveness α_δ decreased from a value of 0.35 at $M = 0.30$ to about 0.29 at $M = 0.89$ (fig. 20).

The variation of lift and drag coefficients with speed at $\delta_e = 0^\circ$ is presented in figure 22. These data show that for a given angle of attack, the lift coefficient increased with Mach number, and this effect became more pronounced as the angle of attack was increased within the test range. At $\delta_e = 0^\circ$, increasing the Mach number produced no effect on the

drag coefficient for angles of attack of less than about 5°. For greater angles of attack, C_D increased with Mach number, and this increase became more pronounced as the angle of attack was increased. For an angle of attack of 10°, the drag coefficient increased from about 0.035 at $M = 0.30$ to 0.095 at $M = 0.89$.

Effect of Transition

The model with transition fixed at the 10-percent-chord line was tested at four representative Mach numbers. The effects produced by fixing transition were generally the same at the four values of Mach number tested and figure 23 is presented to show the effects of fixing transition on the aerodynamic characteristics at $M = 0.75$. The test data indicate that fixing transition generally had a very small effect on the model characteristics.

CONCLUSIONS

An investigation was made in the Langley 300 mph and high-speed 7- by 10-foot tunnels of the aerodynamic characteristics of a 45° sweptback, semispan, horizontal tail equipped with a horn-balanced 25-percent-chord elevator. Tests were made of the model at low speed $(M = 0.30)$ to determine the effects of horn size and horn inboard-edge fairing. The model equipped with the horn that gave the best low-speed hinge-moment characteristics was tested through a speed range $(M = 0.30$ to $M = 0.89)$. The results of the investigation led to the following conclusions:

1. At a Mach number of 0.30, the rates of change of hinge-moment coefficient with angle of attack and with elevator deflection C_{h_α} and C_{h_δ} increased positively as the horn-balance area was increased. For a given change in horn size, C_{h_δ} changed approximately five times as much as C_{h_α}

2. The rate of change of lift coefficient with angle of attack C_{L_α} was unaffected by changes in horn size. The rate of change of lift coefficient with elevator deflection C_{L_δ} and the elevator-effectiveness parameter α_δ increased slightly with increasing horn size.

3. Fairing the horn inboard edge had a pronounced unbalancing effect on C_{h_δ}. The changes in C_{h_α} and in the lift parameters were negligible.

4. Although the particular arrangement investigated through the speed range was overbalanced at moderate and high speeds, it is believed that modifications such as a decrease in horn-balance size or a reduction in elevator trailing-edge angle may make the horn type of balance satisfactory up to high subsonic speeds.

5. The increase of lift-curve slope with Mach number is in good agreement with theory. The rate of change of lift coefficient with elevator deflection was unaffected by changes in Mach number for the speed range investigated.

Langley Aeronautical Laboratory
National Advisory Committee for Aeronautics
Langley Field, Va.

REFERENCES

1. Cleary, Joseph W., and Krumm, Walter J.: High-Speed Aerodynamic Characteristics of Horn and Overhang Balances on a Full-Scale Elevator. NACA RM No. A7H29, 1948.

2. Lowry, John G.: Résumé of Hinge-Moment Data for Unshielded Horn-Balanced Control Surfaces. NACA RB No. 3F19, 1943.

3. Thomas, H. H. B. M., and Lofts, M.: Analysis of Wind Tunnel Data on Horn Balance. Rep. No. Aero 1994, British R.A.E., Nov. 1944.

4. Lowry, John G., Maloney, James A., and Garner, I. Elizabeth: Wind-Tunnel Investigation of Shielded Horn Balances and Tabs on a 0.7-Scale Model of XF6F Vertical Tail Surface. NACA ACR No. 4C11, 1944.

5. Becker, John V., and Cooper, Morton: Structural Hinge-Moment Increments Caused by Hinge-Axis Distortion. NACA TN No. 1038, 1946.

6. Swanson, Robert S., and Toll, Thomas A.: Jet-Boundary Corrections for Reflection-Plane Models in Rectangular Wind Tunnels. NACA Rep. No. 770, 1943.

7. Herriot, John G.: Blockage Corrections for Three-Dimensional-Flow Closed-Throat Wind Tunnels, with Consideration of the Effect of Compressibility. NACA RM No. A7B28, 1947.

8. Toll, Thomas A., and Schneiter, Leslie E.: Approximate Relations for Hinge-Moment Parameters of Control Surfaces on Swept Wings at Low Mach Numbers. NACA TN No. 1711, 1948.

9. Axelson, John A.: A Summary and Analysis of Wind-Tunnel Data on the Lift and Hinge-Moment Characteristics of Control Surfaces up to a Mach Number of 0.90. NACA RM No. A7L02, 1947.

10. DeYoung, John: Theoretical Additional Span Loading Characteristics of Wings with Arbitrary Sweep, Aspect Ratio, and Taper Ratio. NACA TN No. 1491, 1947.

TABLE I.– HORN DIMENSIONS

Horn	Horn span, (in.) (a)	Average chord, (in.) (b)	Area, (sq in.)	Balance coefficient, B
Large	7.42	4.06	30.13	0.44
Intermediate	6.42	3.53	22.66	.36
Faired	6.42	3.53	22.66	.36
Small	5.42	2.99	16.20	.28

[a]Measured parallel to hinge line.

[b]Measured normal to hinge line.

TABLE II.– SUMMARY OF THE AERODYNAMIC CHARACTERISTICS

[M = 0.30]

Horn	B	C_{h_α}	C_{h_δ}	C_{L_α}	C_{L_δ}	α_δ
Large	0.44	0.0012	0.0075	0.0440	0.0195	0.443
Intermediate	.36	–.0003	.0025	.0430	.0165	.384
Faired	.36	0	–.0014	.0430	.0165	.384
Small	.28	–.0010	–.0024	.0430	.0160	.372

NACA

[redacted]

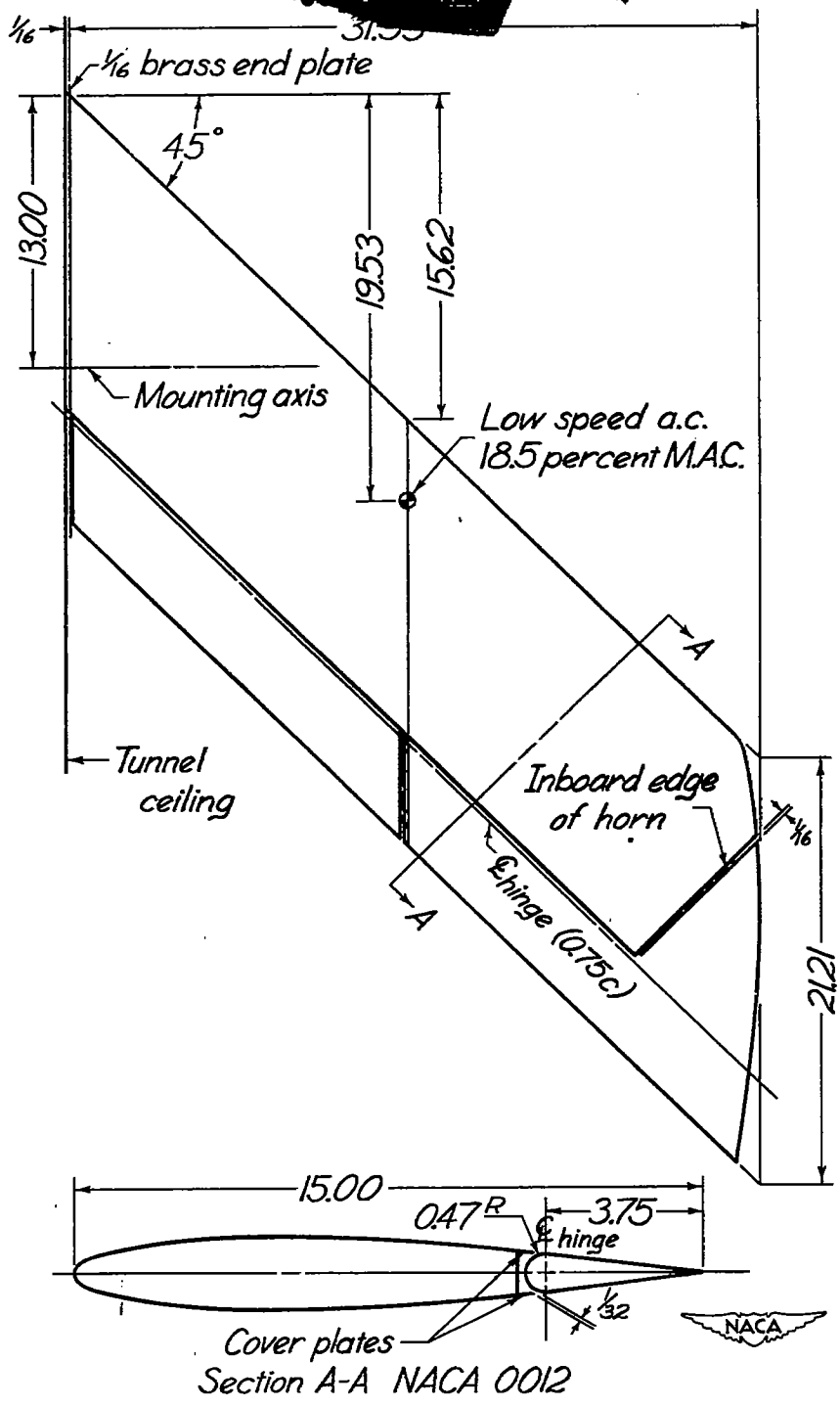

Figure 1.- Drawing of the 45° sweptback semispan horizontal-tail model equipped with the large horn. (All dimensions are in inches.)

[redacted]

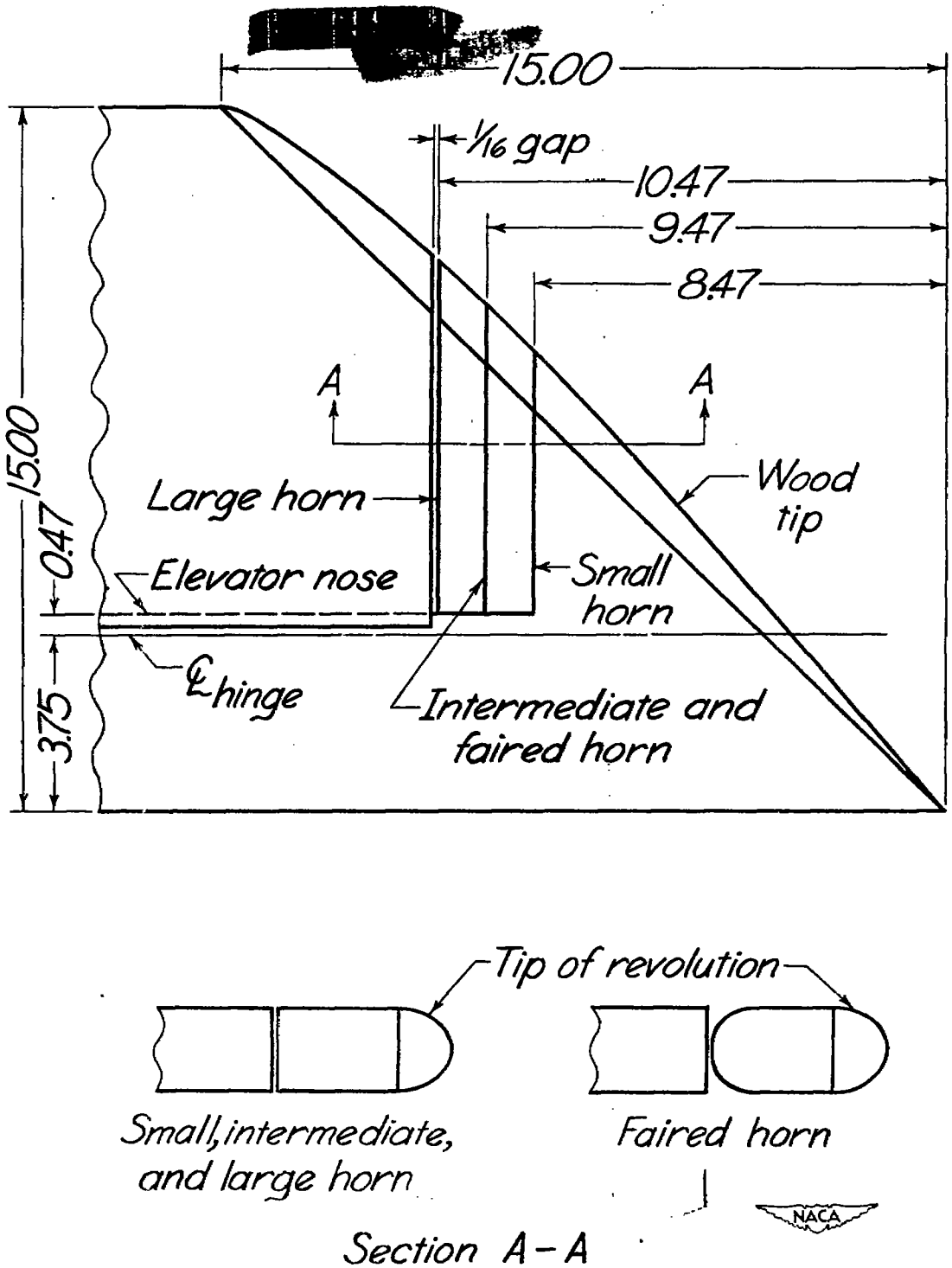

Figure 2.- Dimensions of the various horn balances used for tests of the 45° sweptback horizontal-tail model. (All dimensions are in inches.)

[redacted]

[redacted]

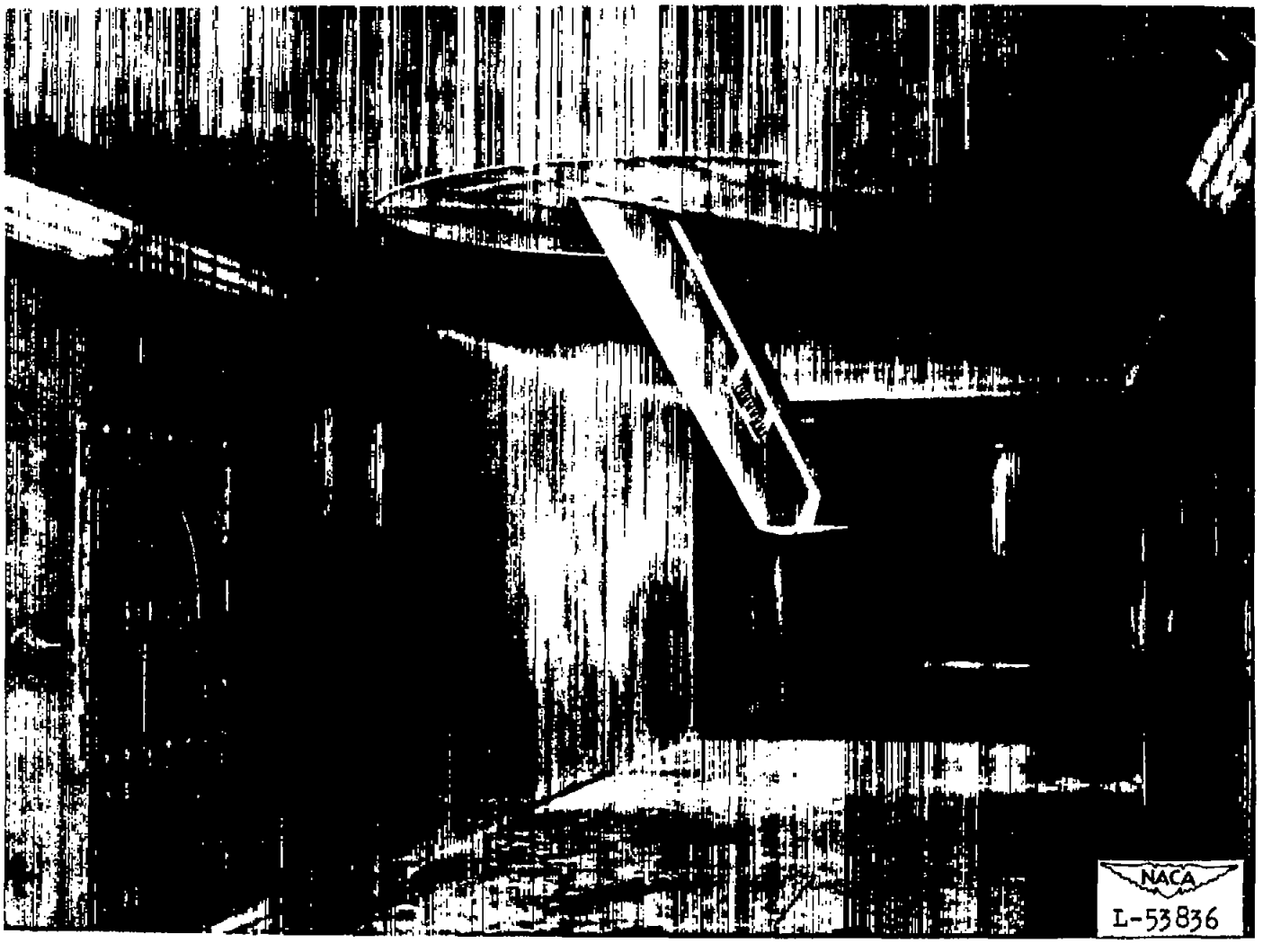

Figure 3.- Photograph of the 45° sweptback horizontal-tail model mounted in the Langley 7- by 10-f[redacted] tunnel.

[redacted]

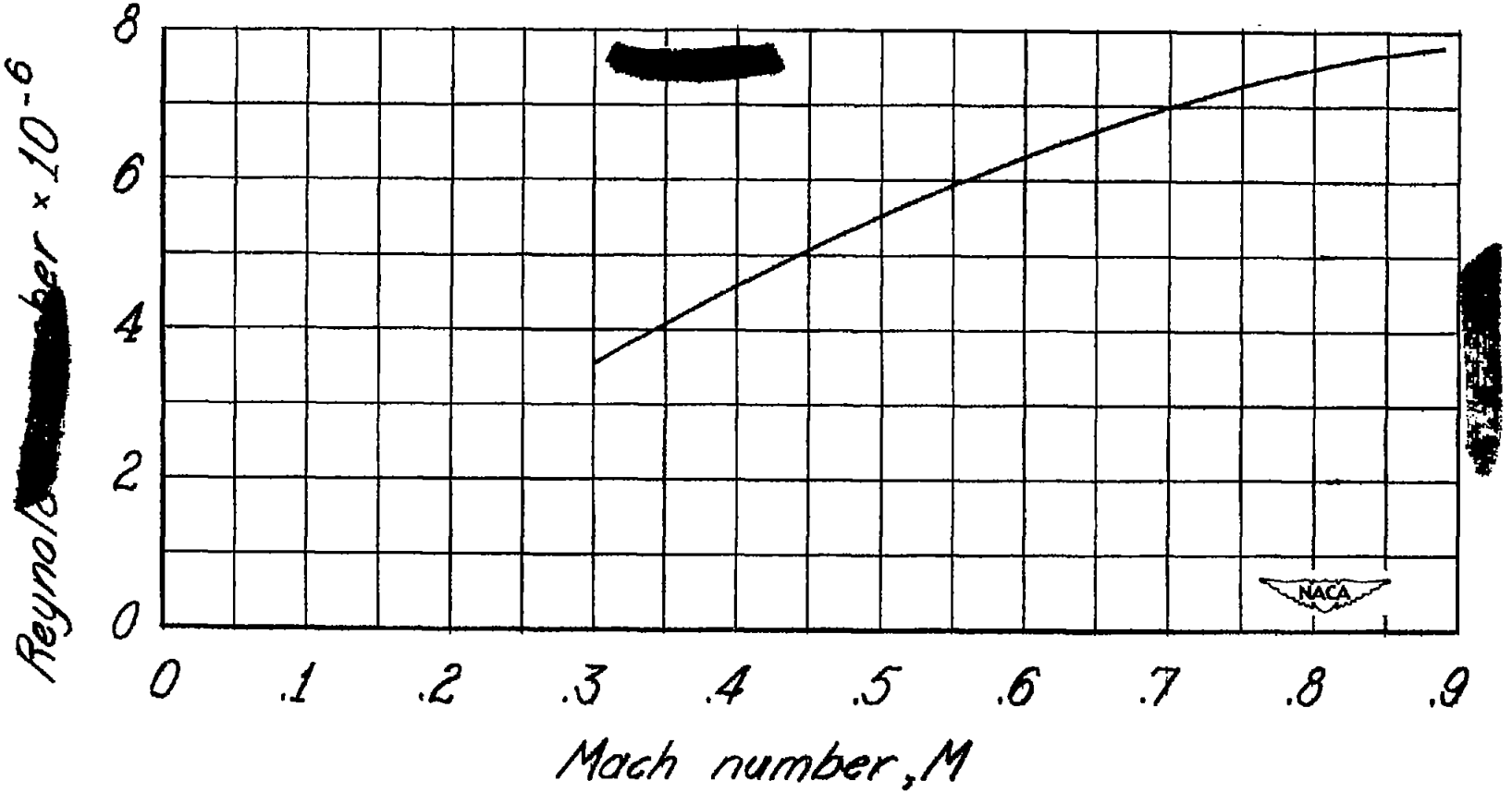

Figure 4.- Variation of average Reynolds number with Mach number.

[redacted]

[redacted]

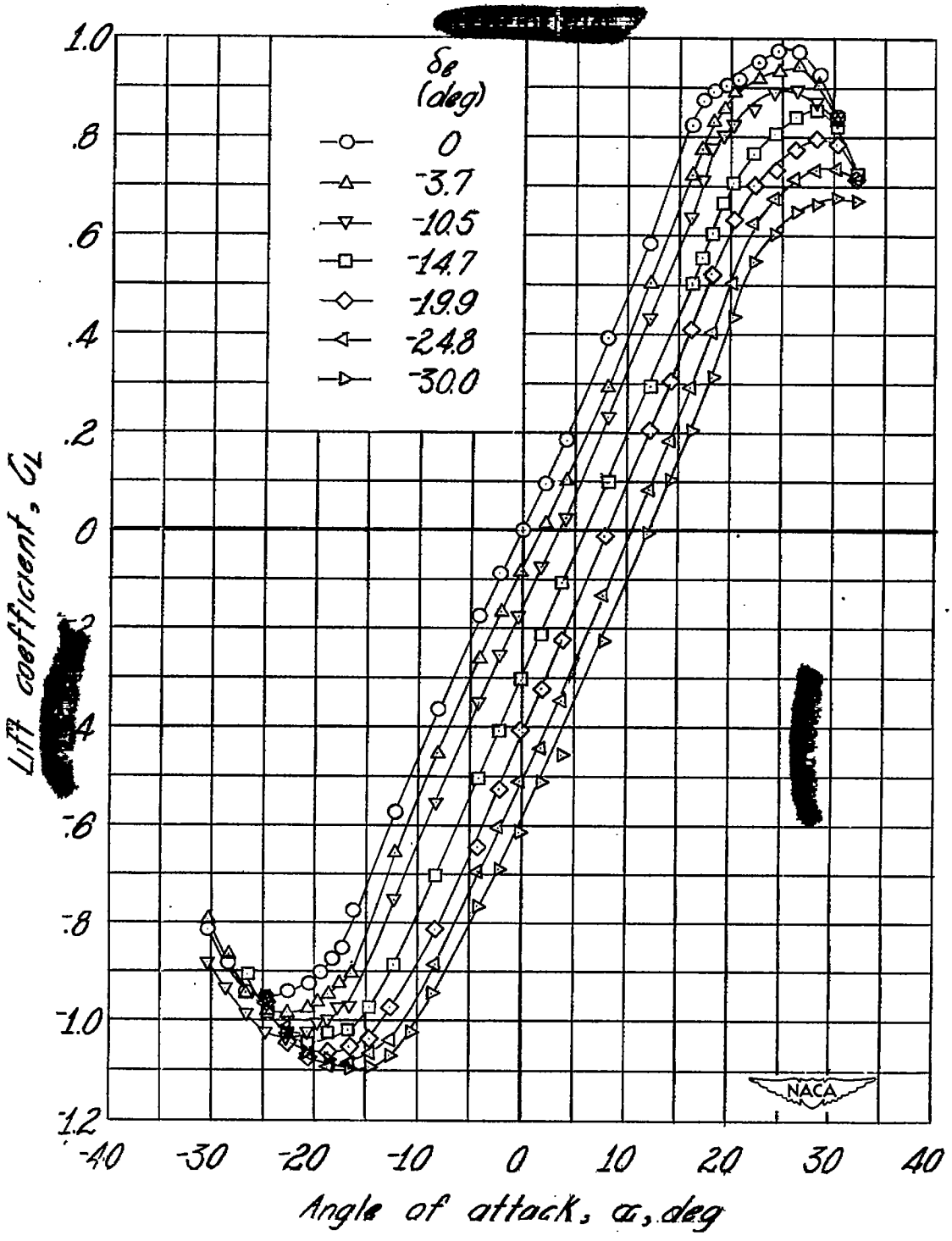

Figure 5.- Aerodynamic characteristics of the 45° sweptback horizontal-tail model equipped with the large horn. M = 0.30.

[redacted]

[redacted]

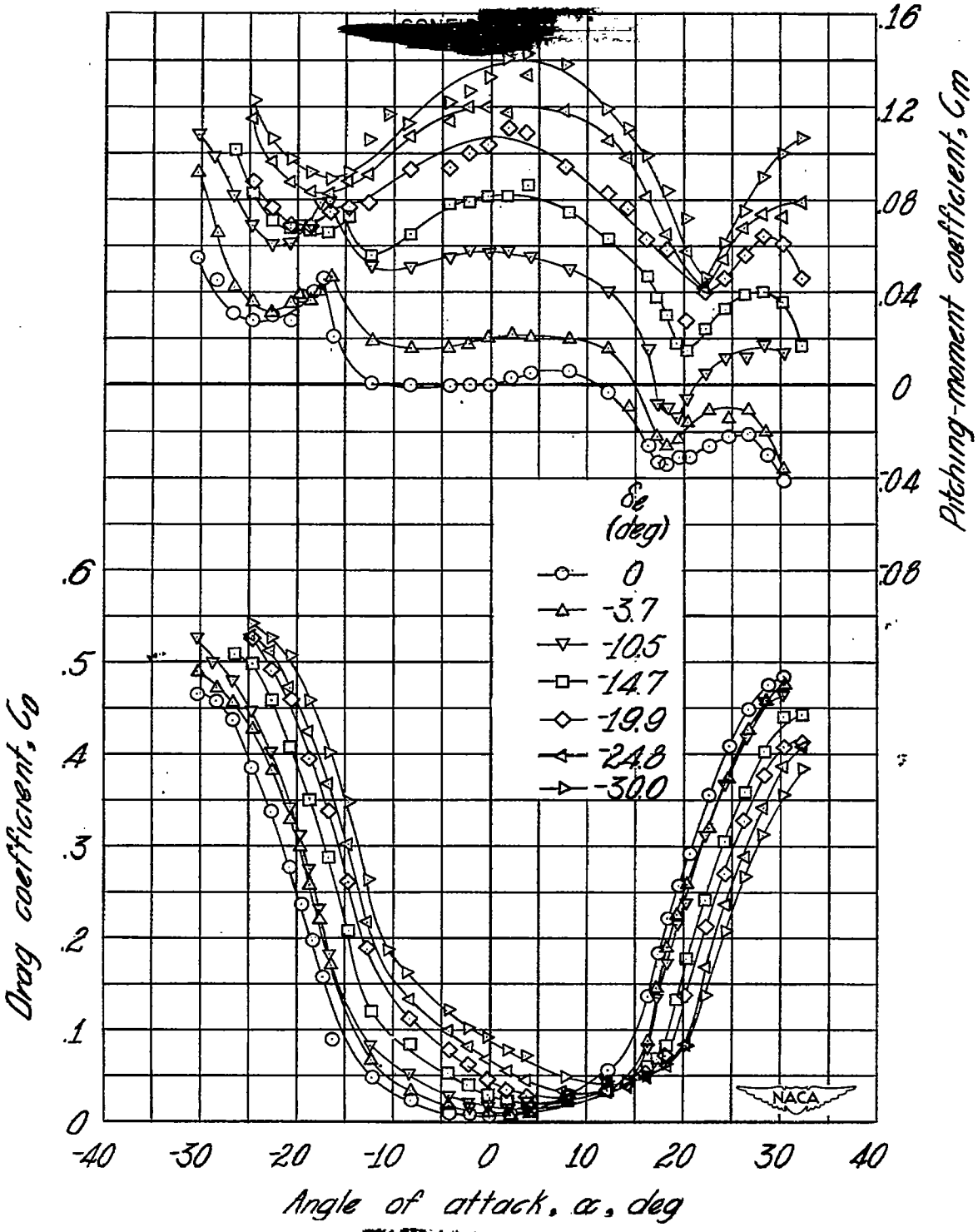

[redacted]

Figure 5.- Continued.

[redacted]

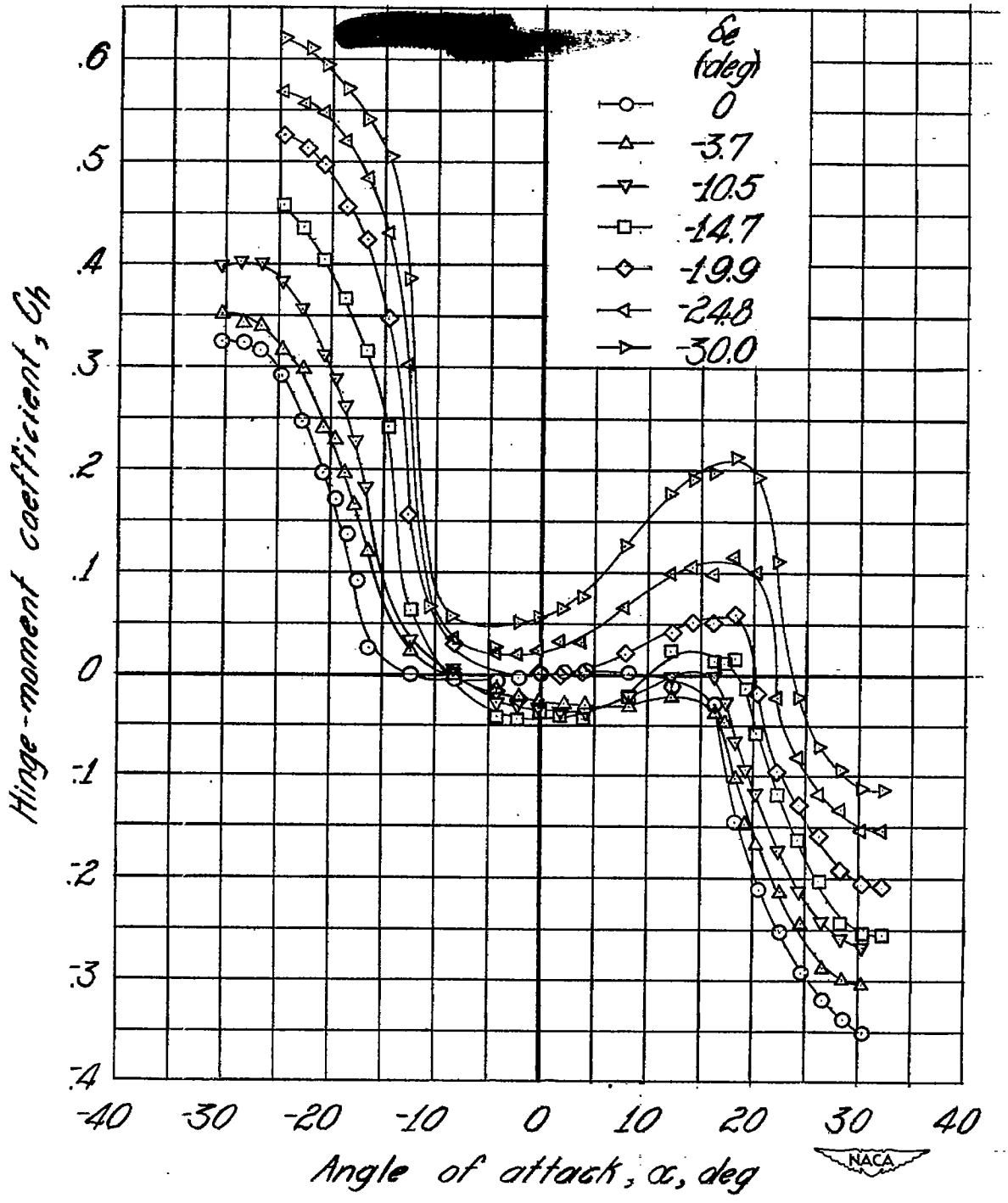

Figure 5.- Concluded.

[redacted]

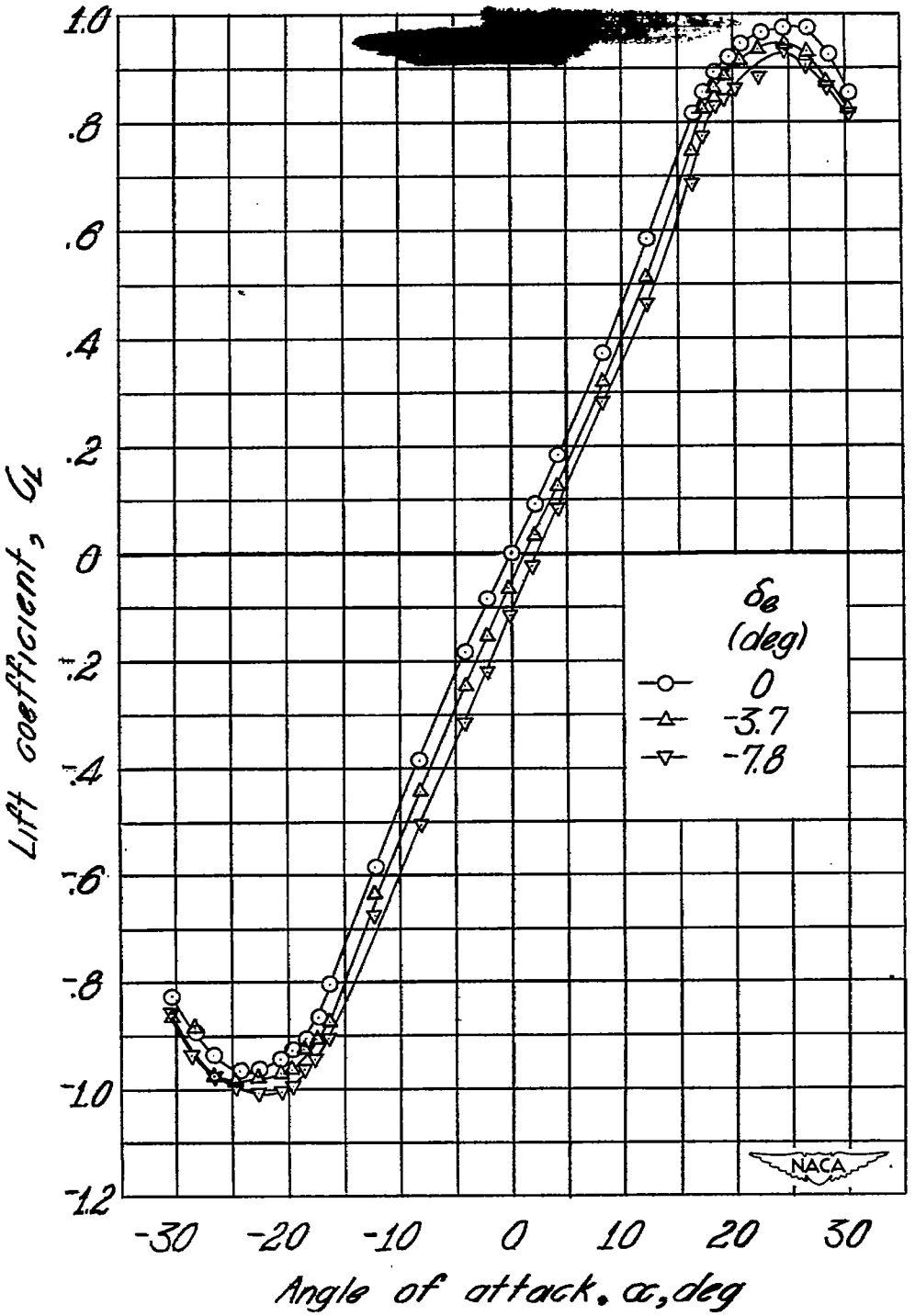

Figure 6.- Aerodynamic characteristics of the 45° sweptback horizontal-tail model equipped with the intermediate horn. M = 0.30.

[redacted]

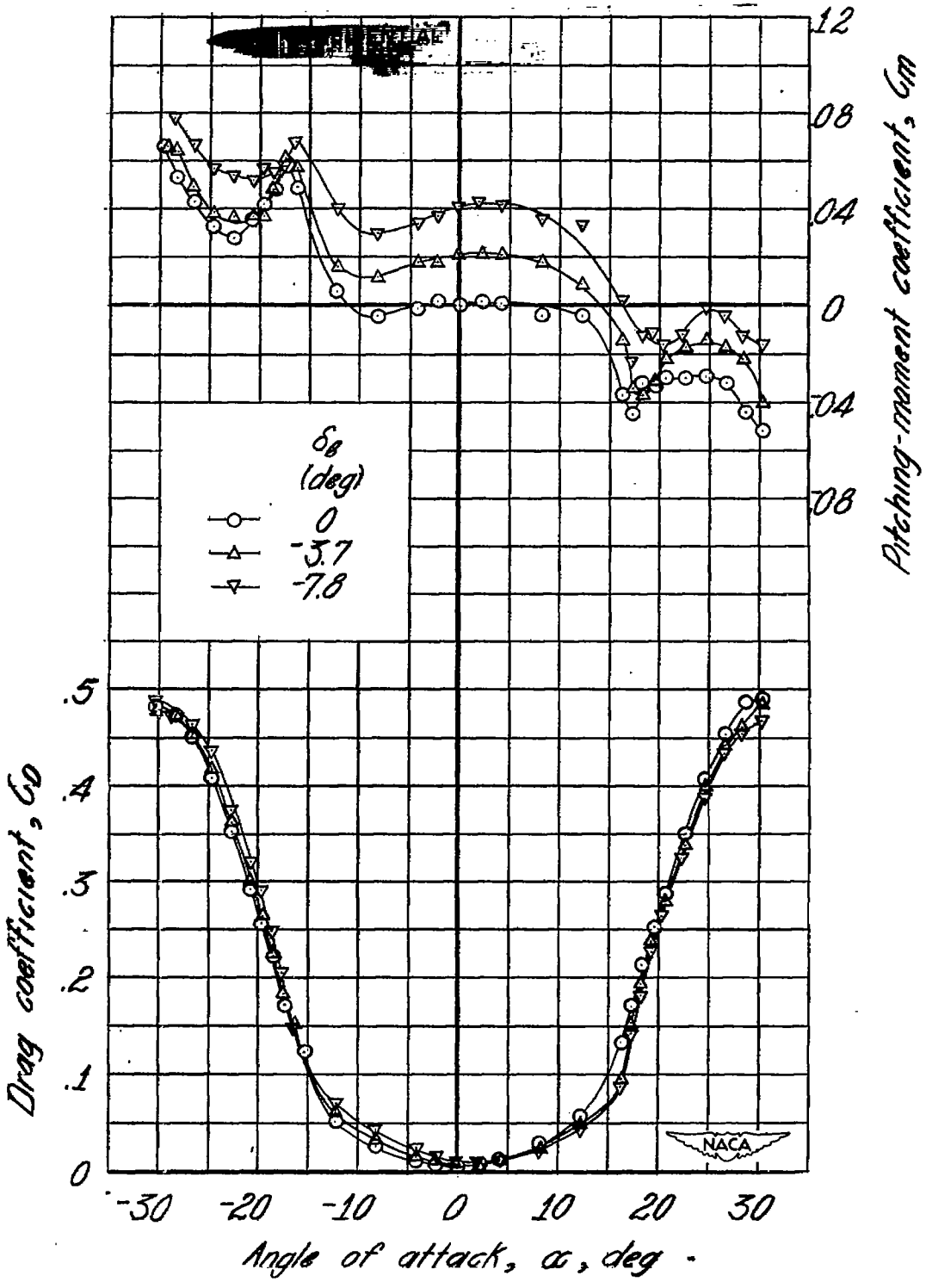

Figure 6.- Continued.

[redacted]

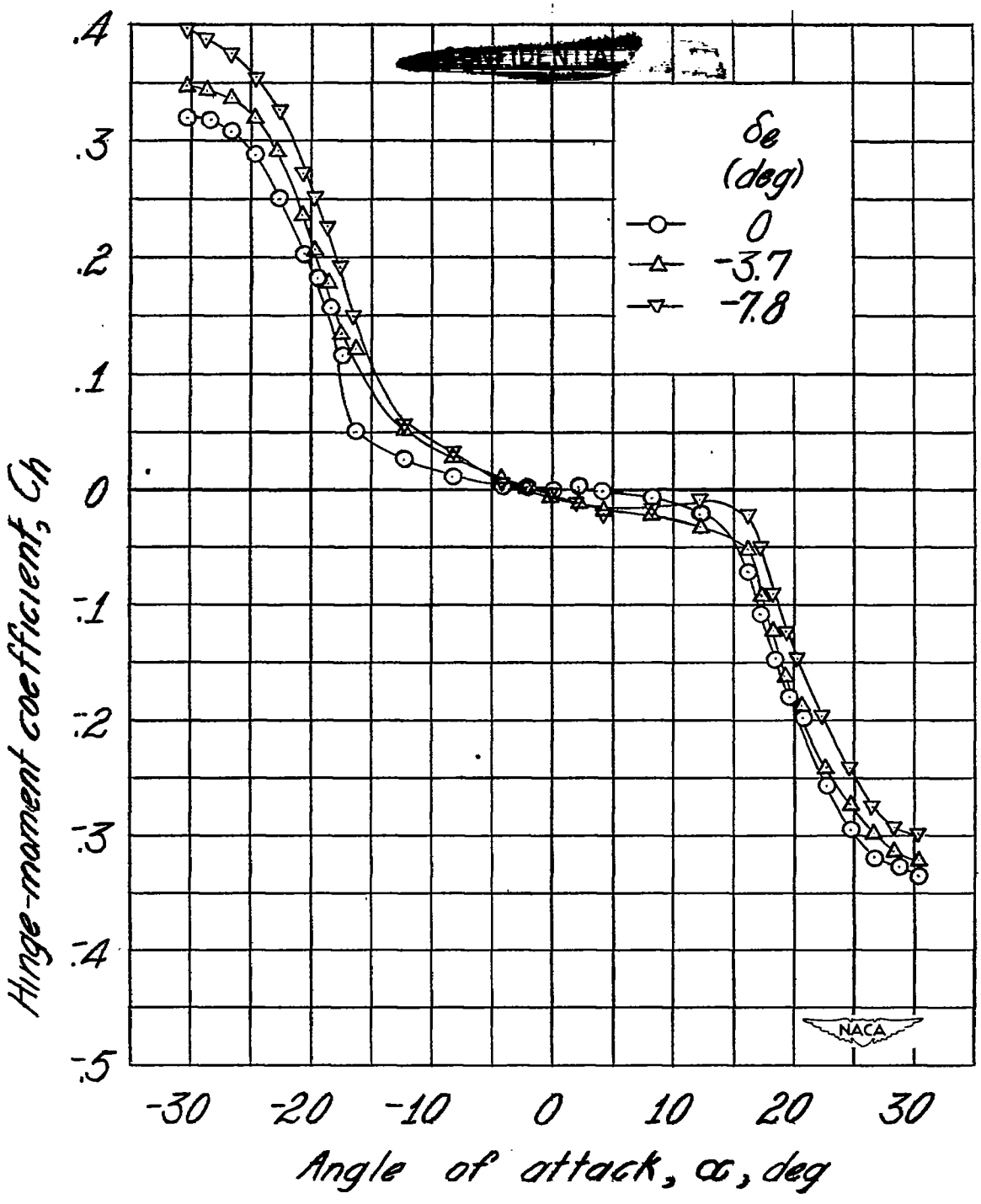

Figure 6.- Concluded.

[redacted]

[redacted]

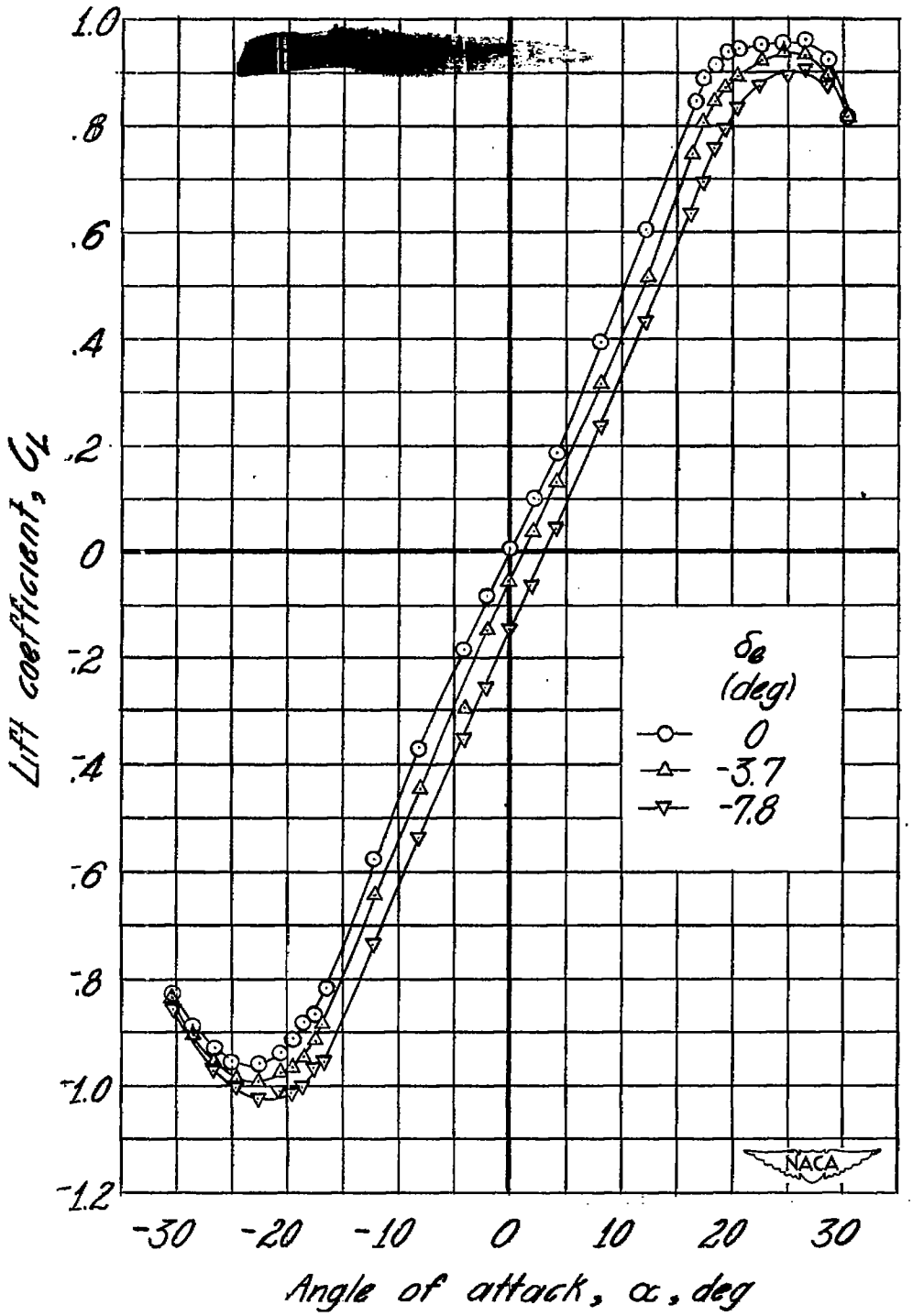

Figure 7.- Aerodynamic char[redacted] the 45° sweptback horizontal-tail model equipped with the small horn. M = 0.30.

[redacted]

[redacted]

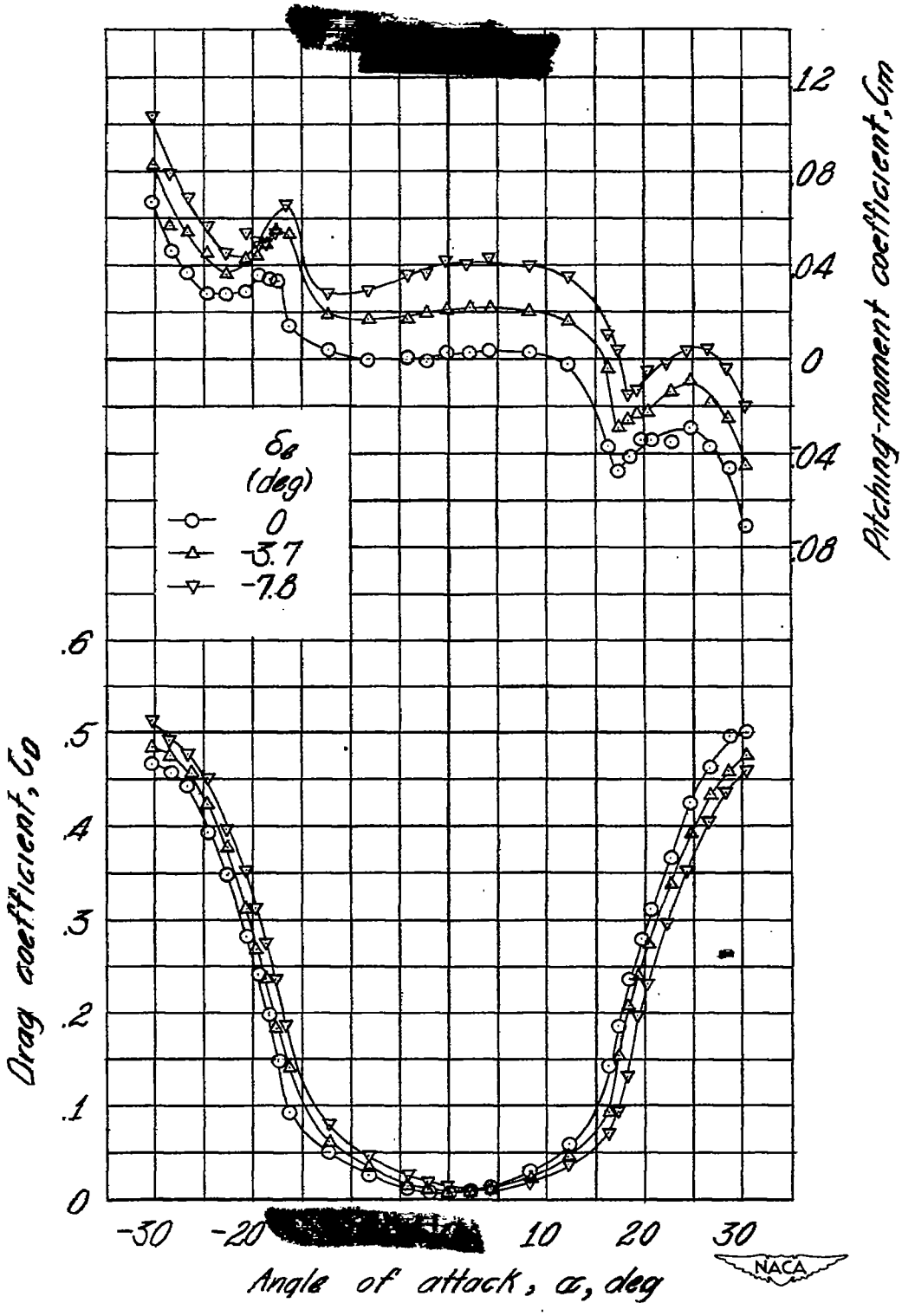

Figure 7.- Continued.

[redacted]

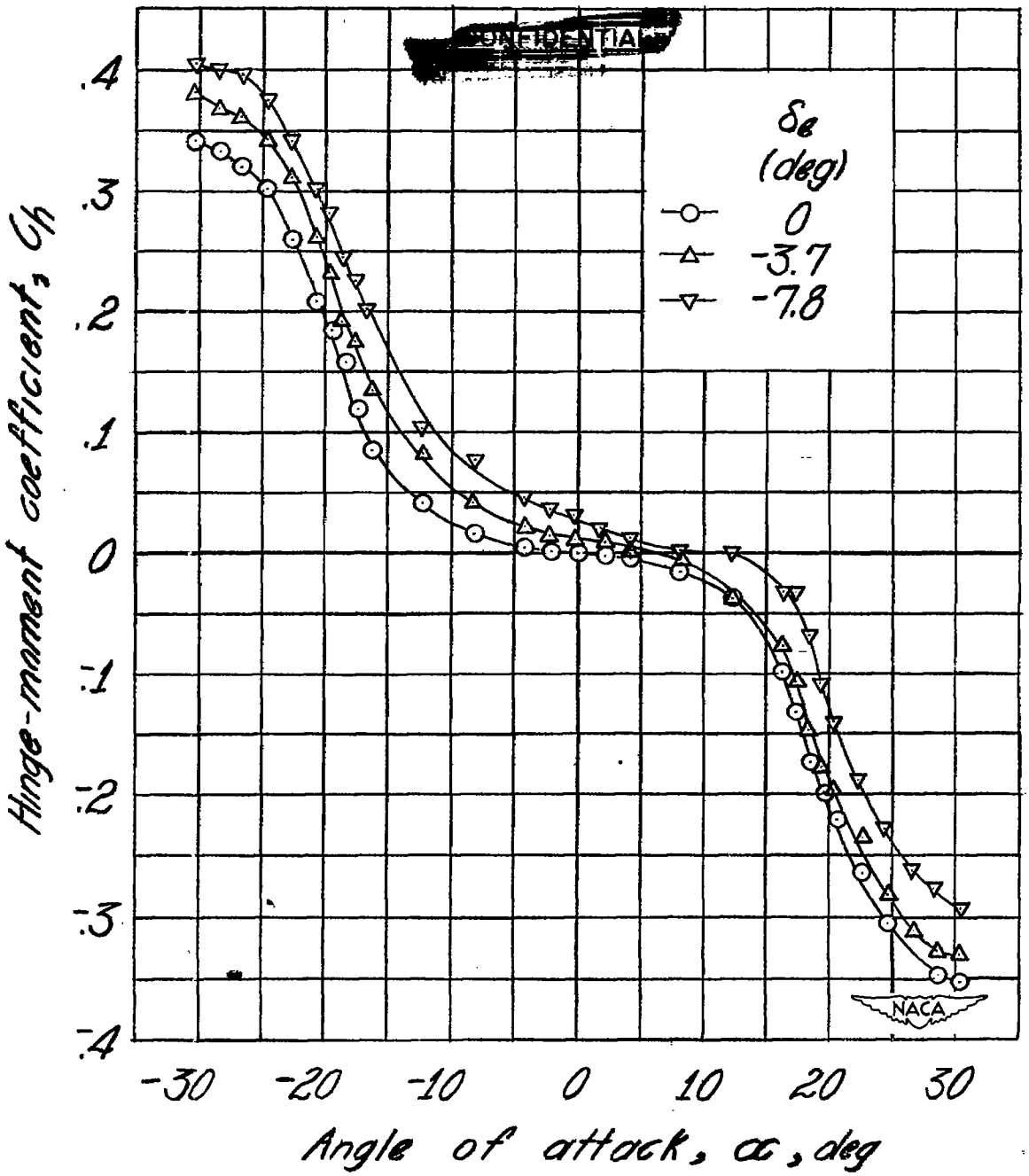

Figure 7.- Concluded.

[redacted]

[redacted]

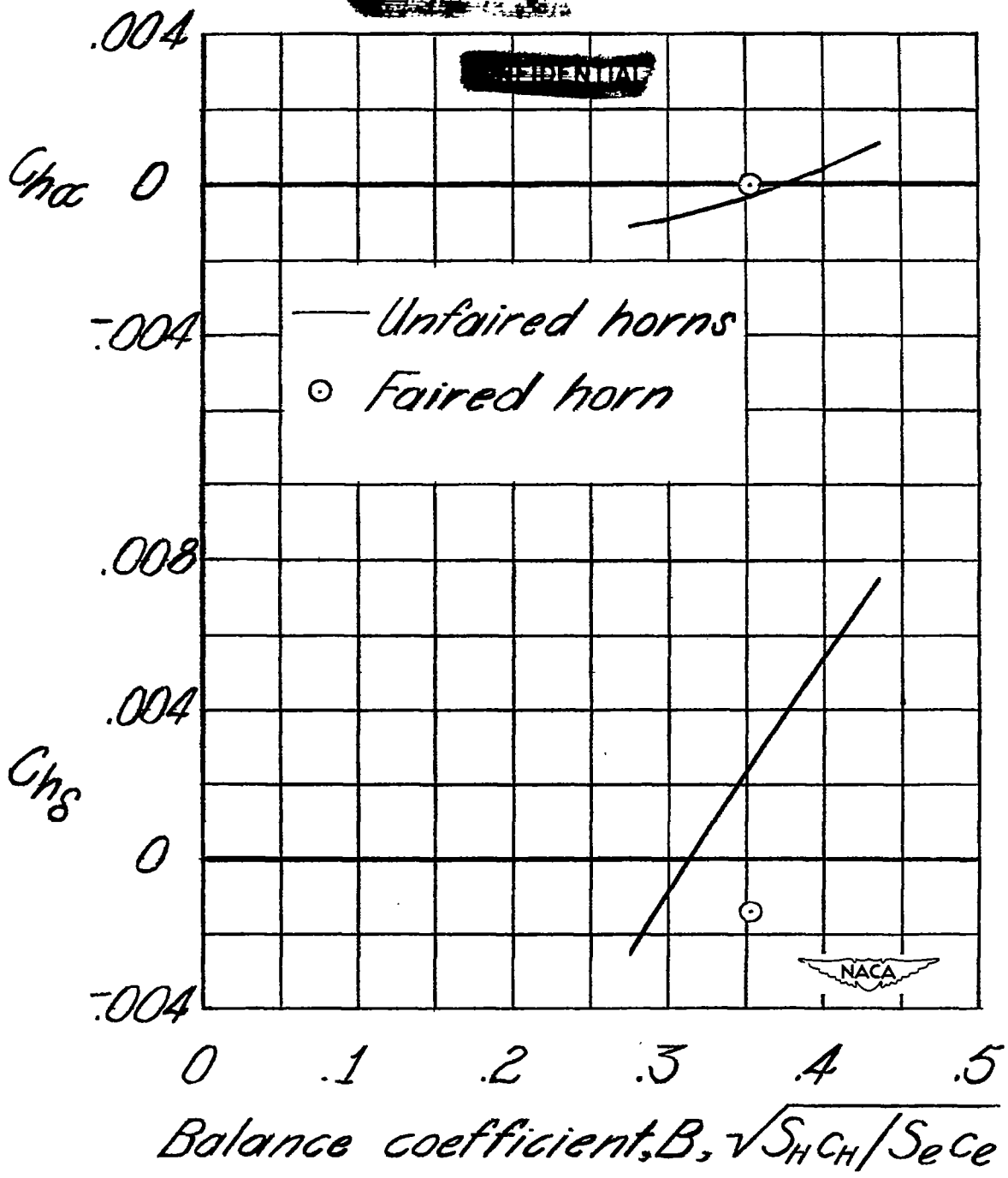

Figure 8.- Variation of the hinge-moment parameters with horn balance coefficient. M = 0.30.

[redacted]

[redacted]

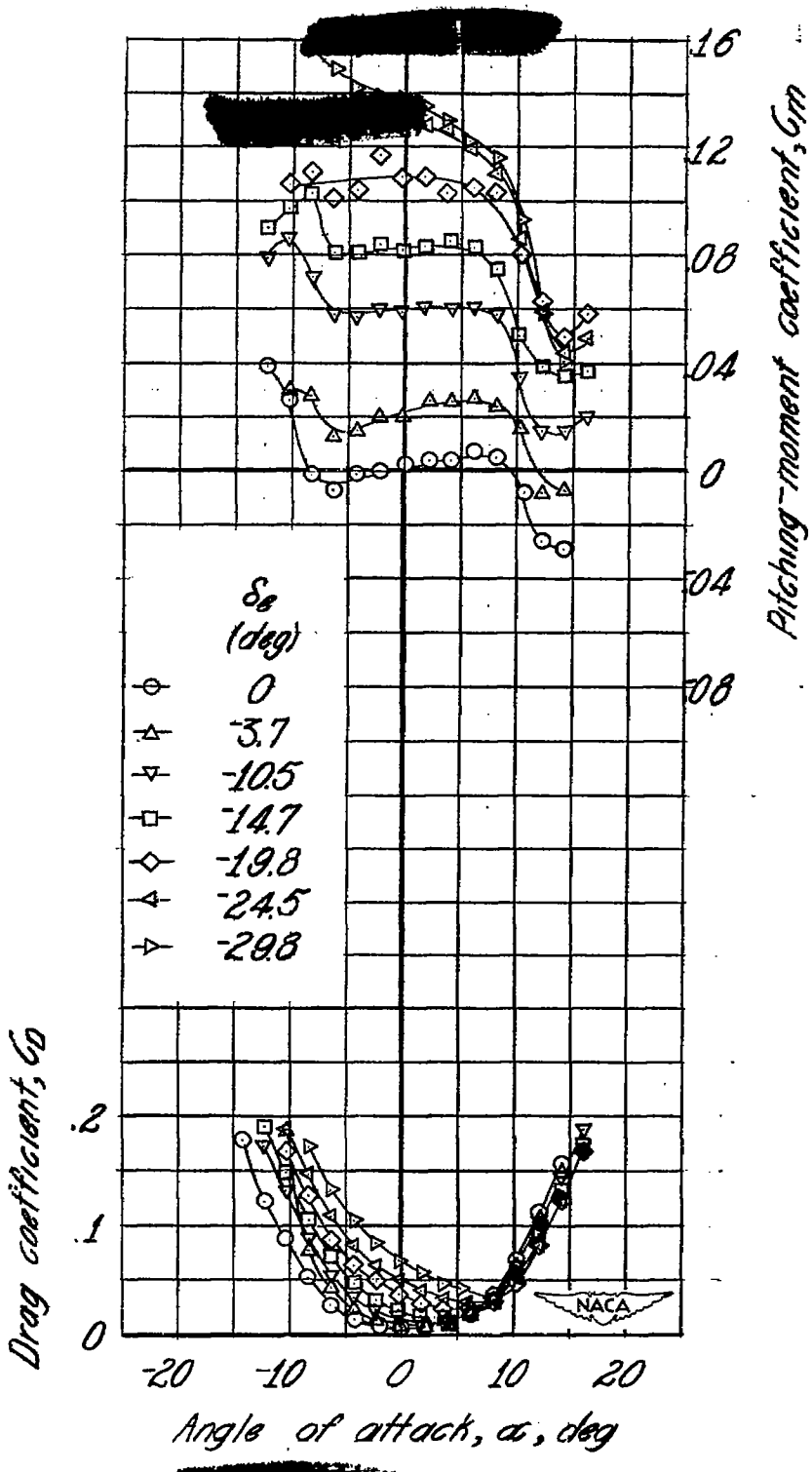

[redacted]inued.

[redacted]

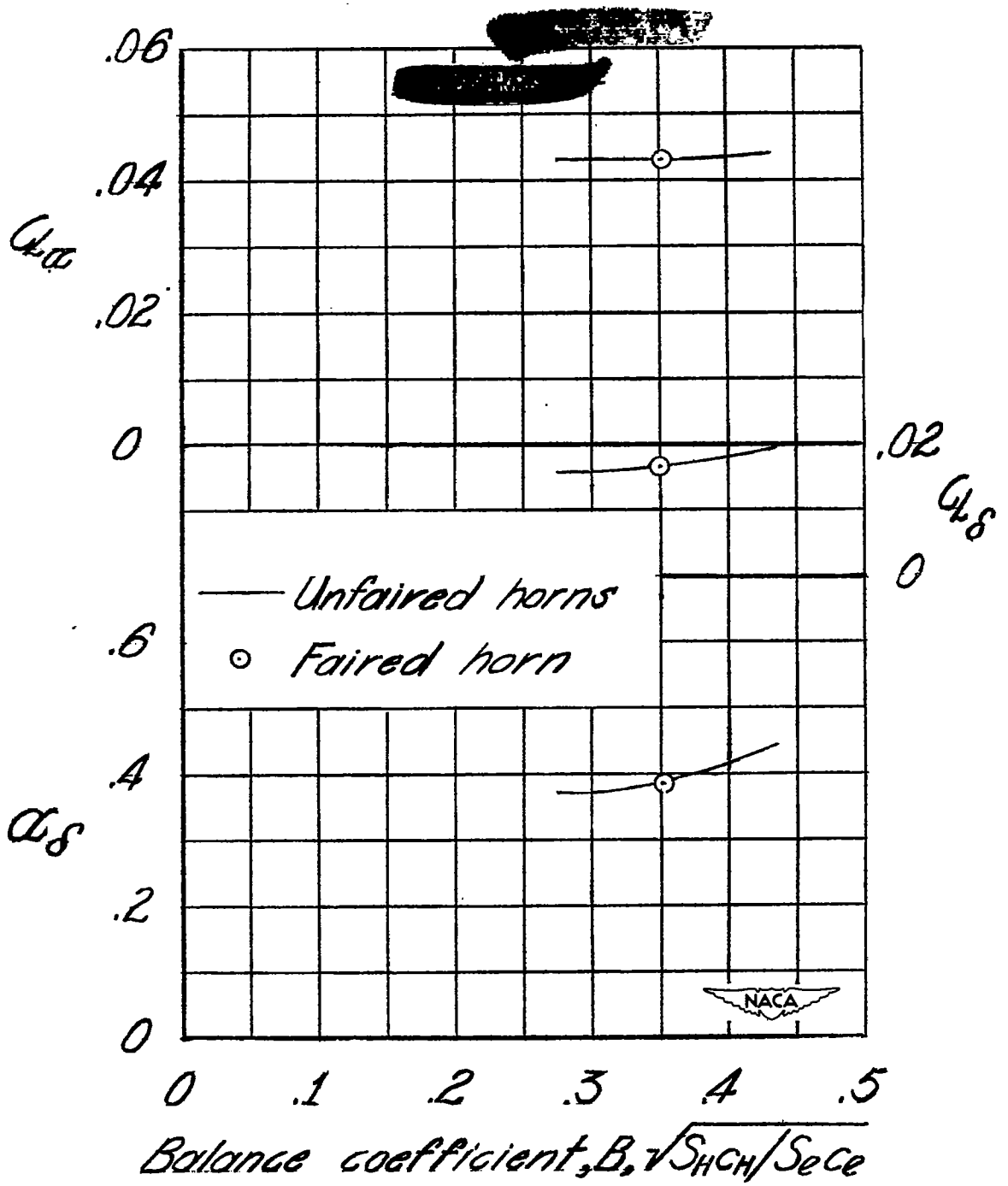

Figure 9.- Variation of the lift parameters with horn balance coefficient. M = 0.30.

[redacted]

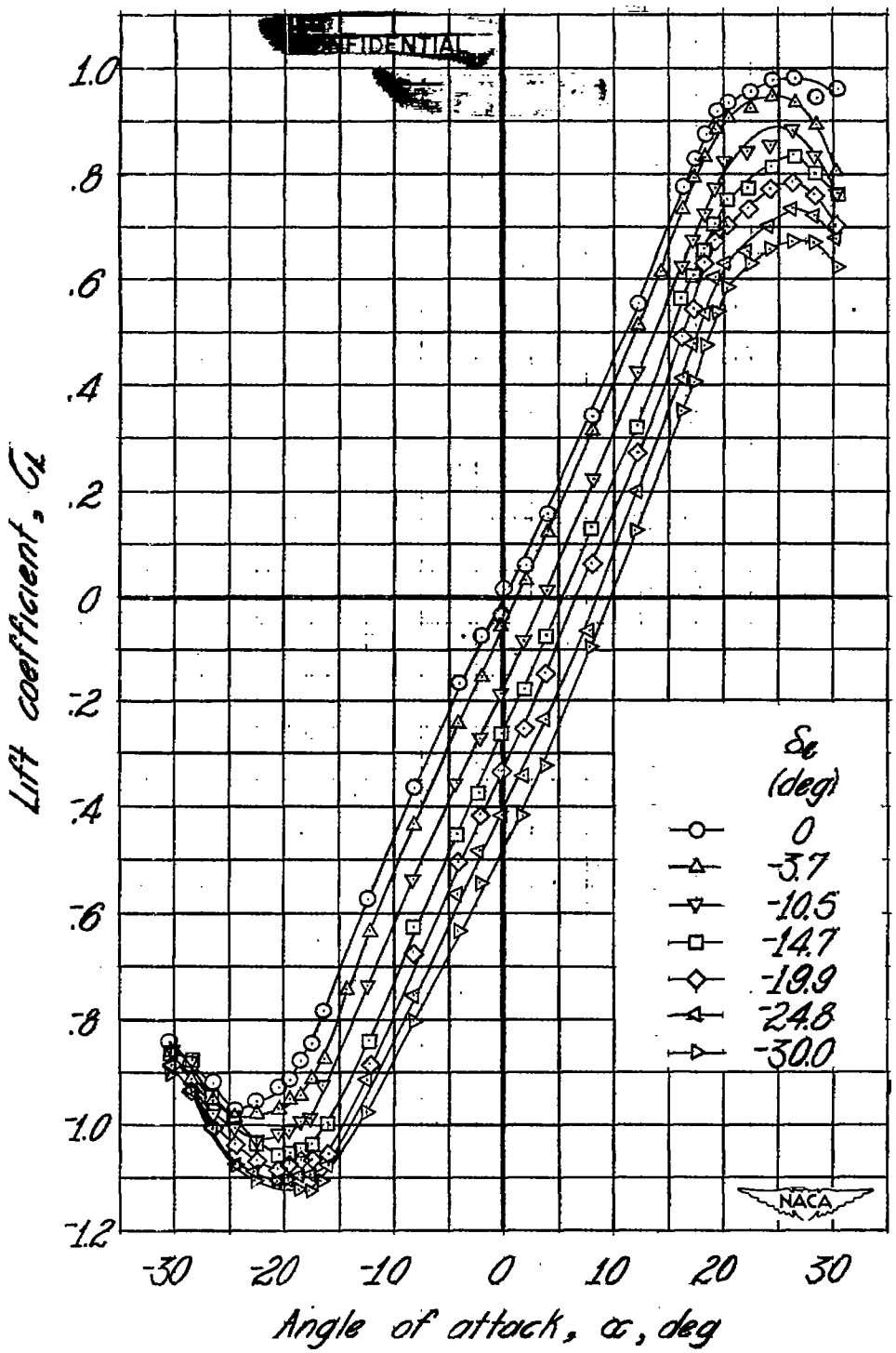

Figure 10.- Aerodynamic characteristics of the 45° sweptback horizontal-tail model equipped with the faired horn. M = 0.30.

[redacted]

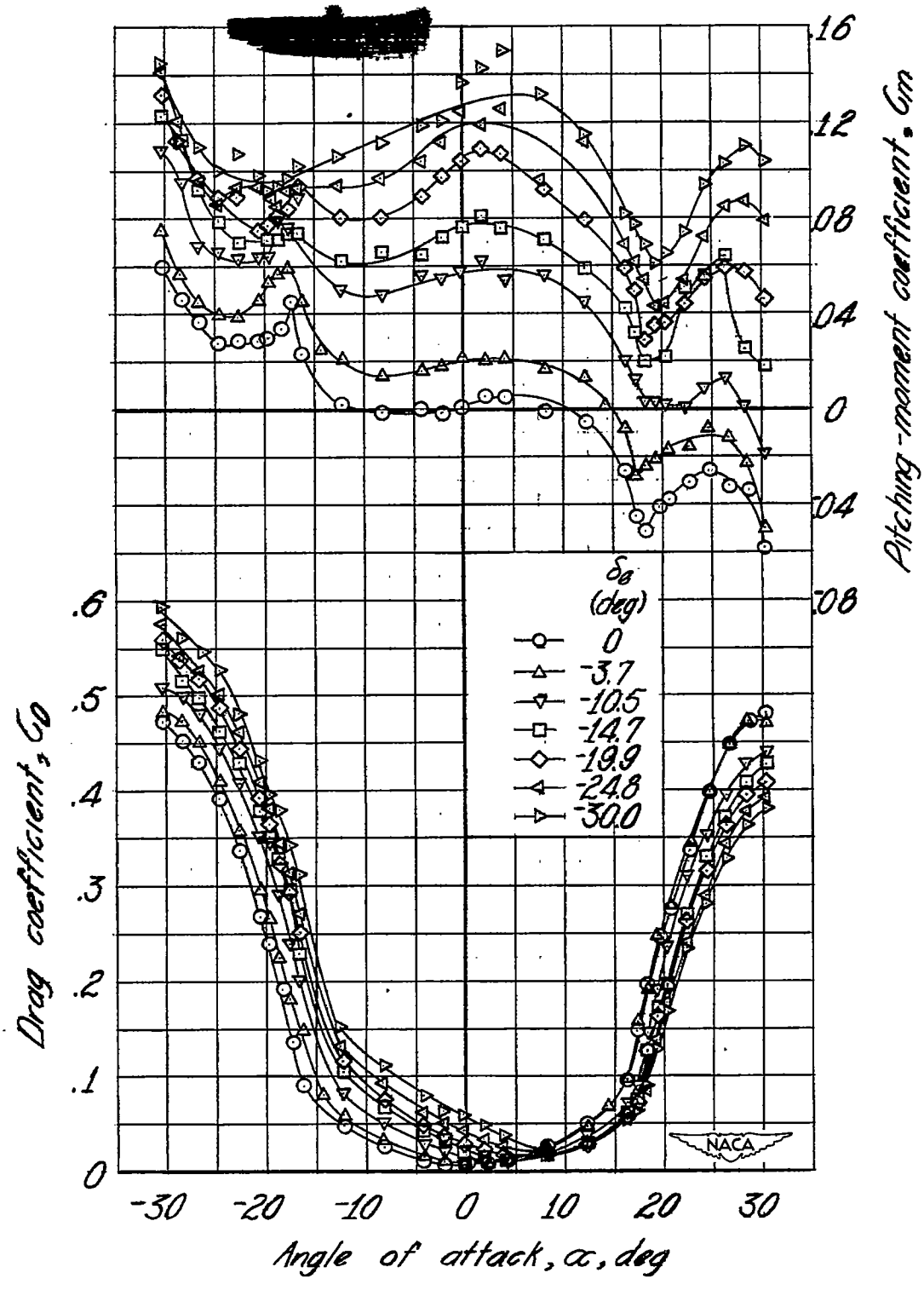

Figure 10.- Continued.

[redacted]

[redacted]

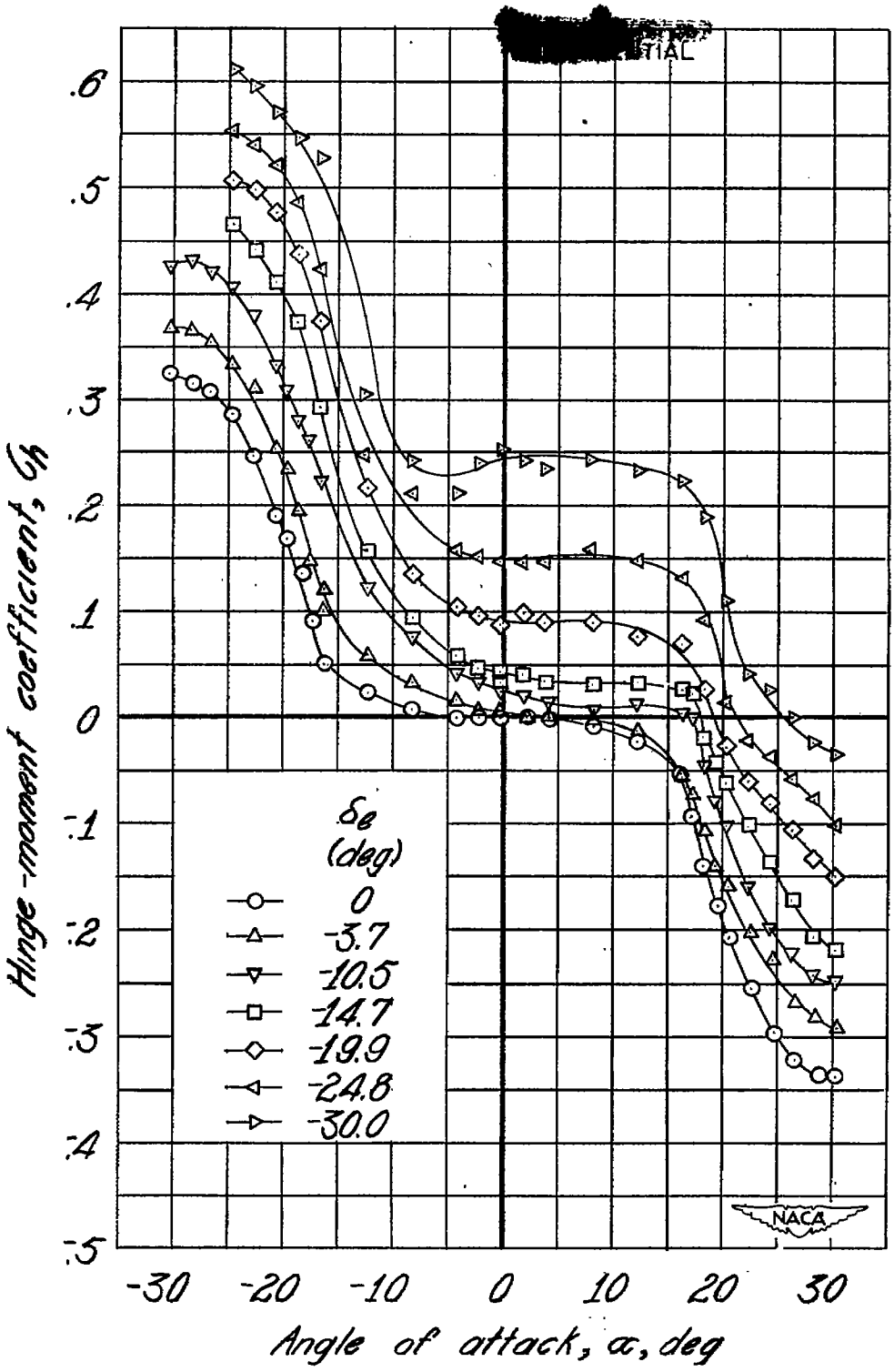

Figure 10.- Concluded.

[redacted]

[redacted]

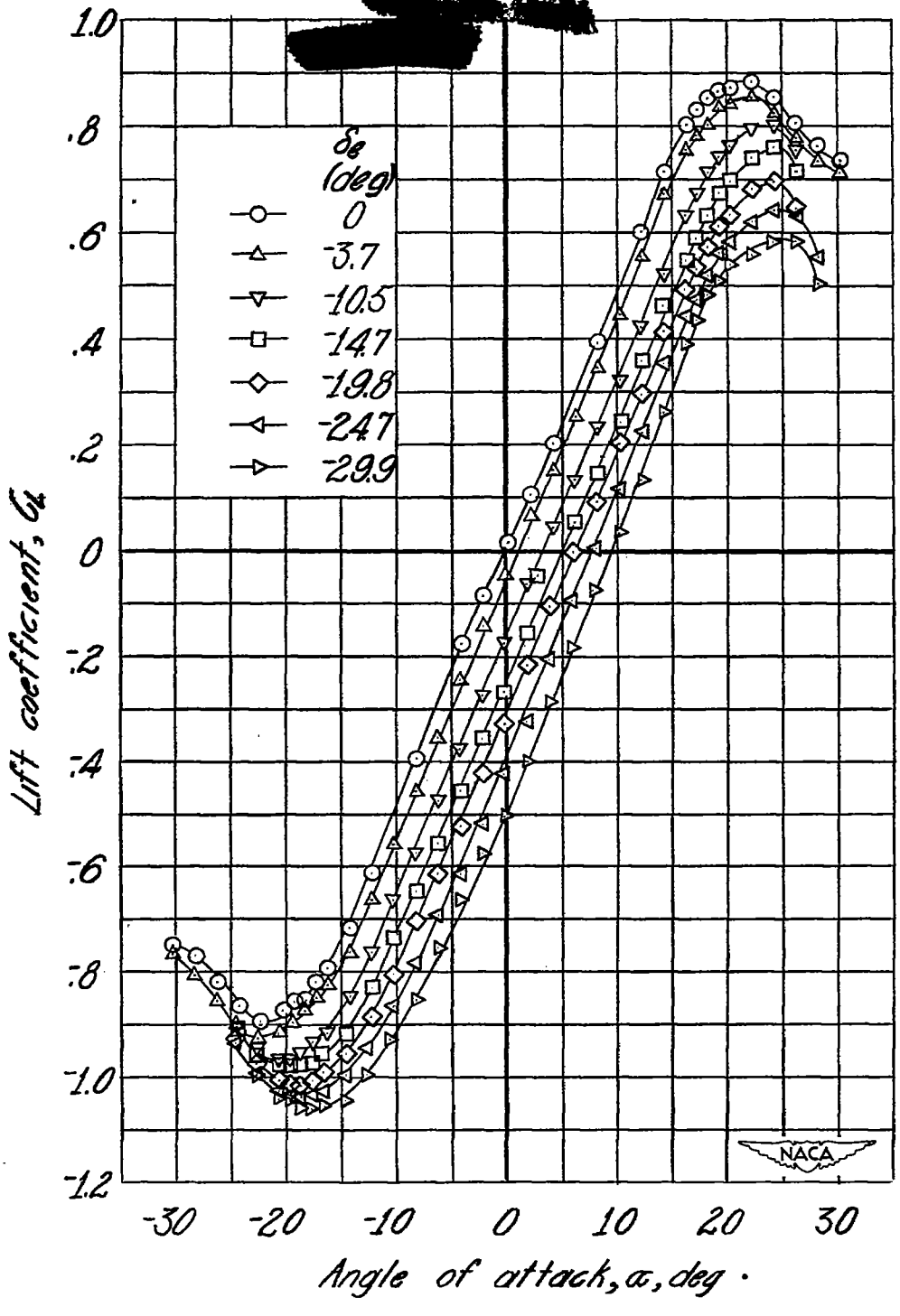

Figure 11.- Aerodynamic characteristics of the 45° sweptback horizontal-tail model equipped with the faired horn. M = 0.50.

[redacted]

[redacted]

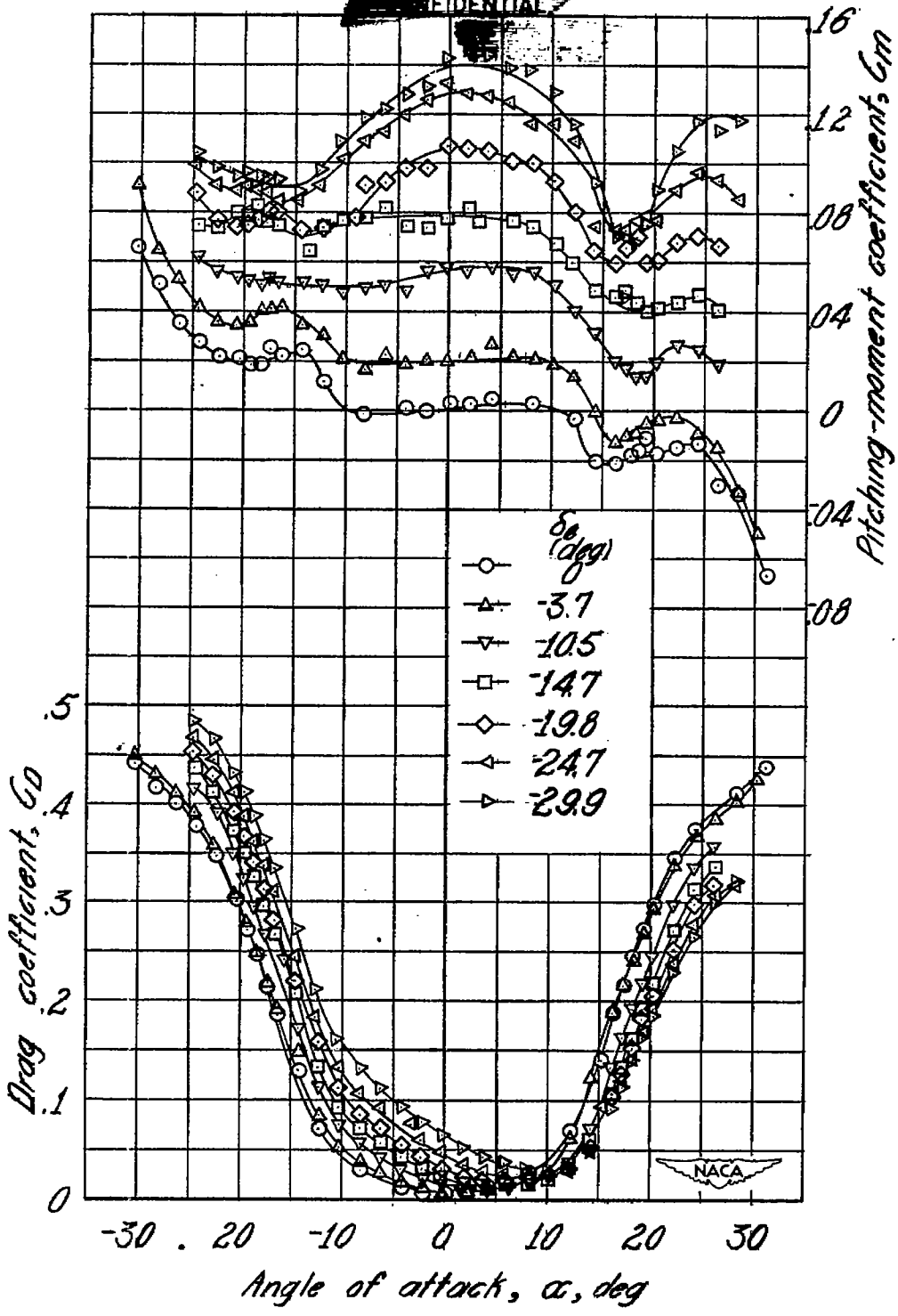

Figure 11.- Continued.

CONFIDENTIAL
[redacted]

[redacted]

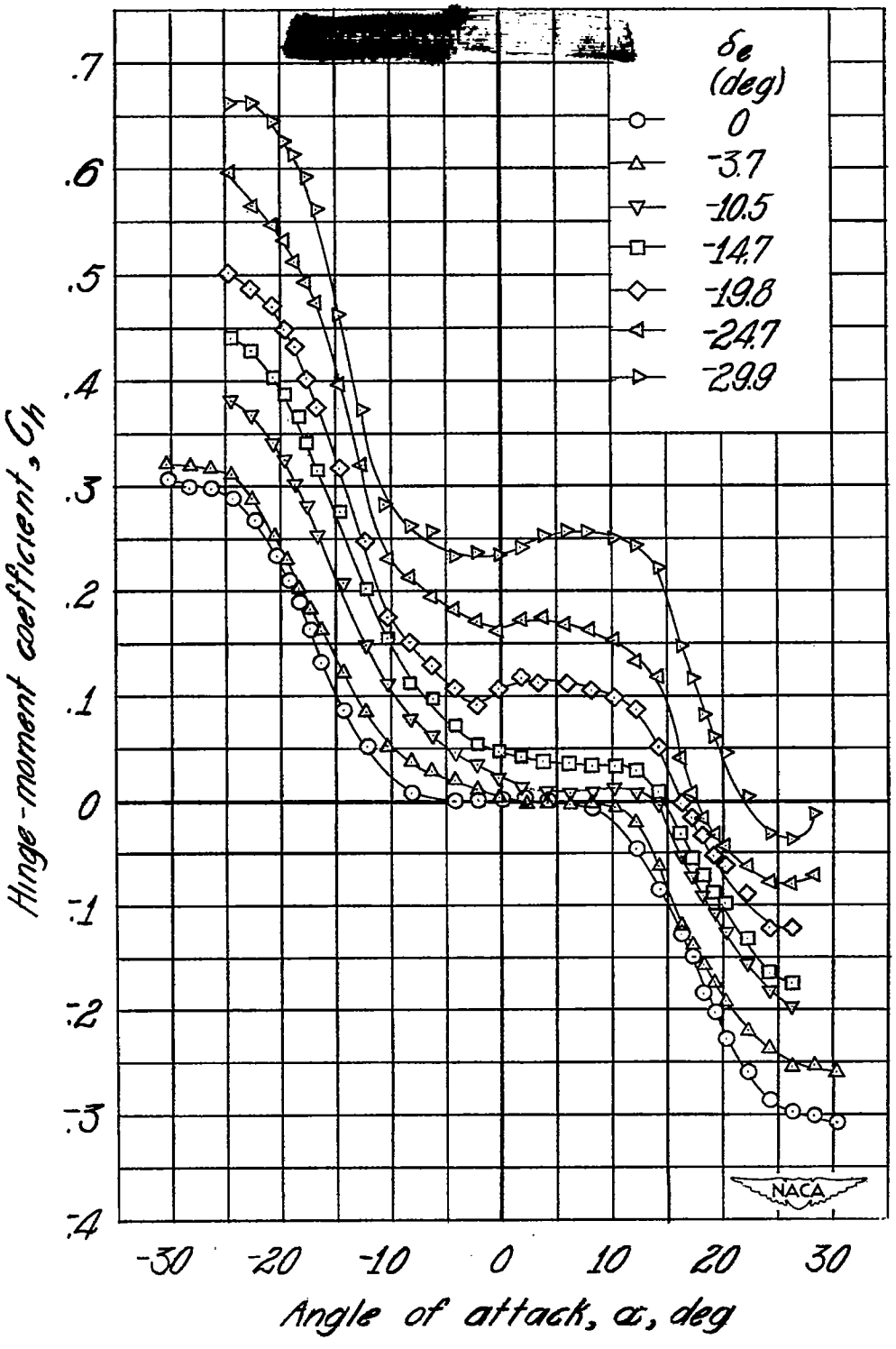

Figure 11.- Concluded.

[redacted]

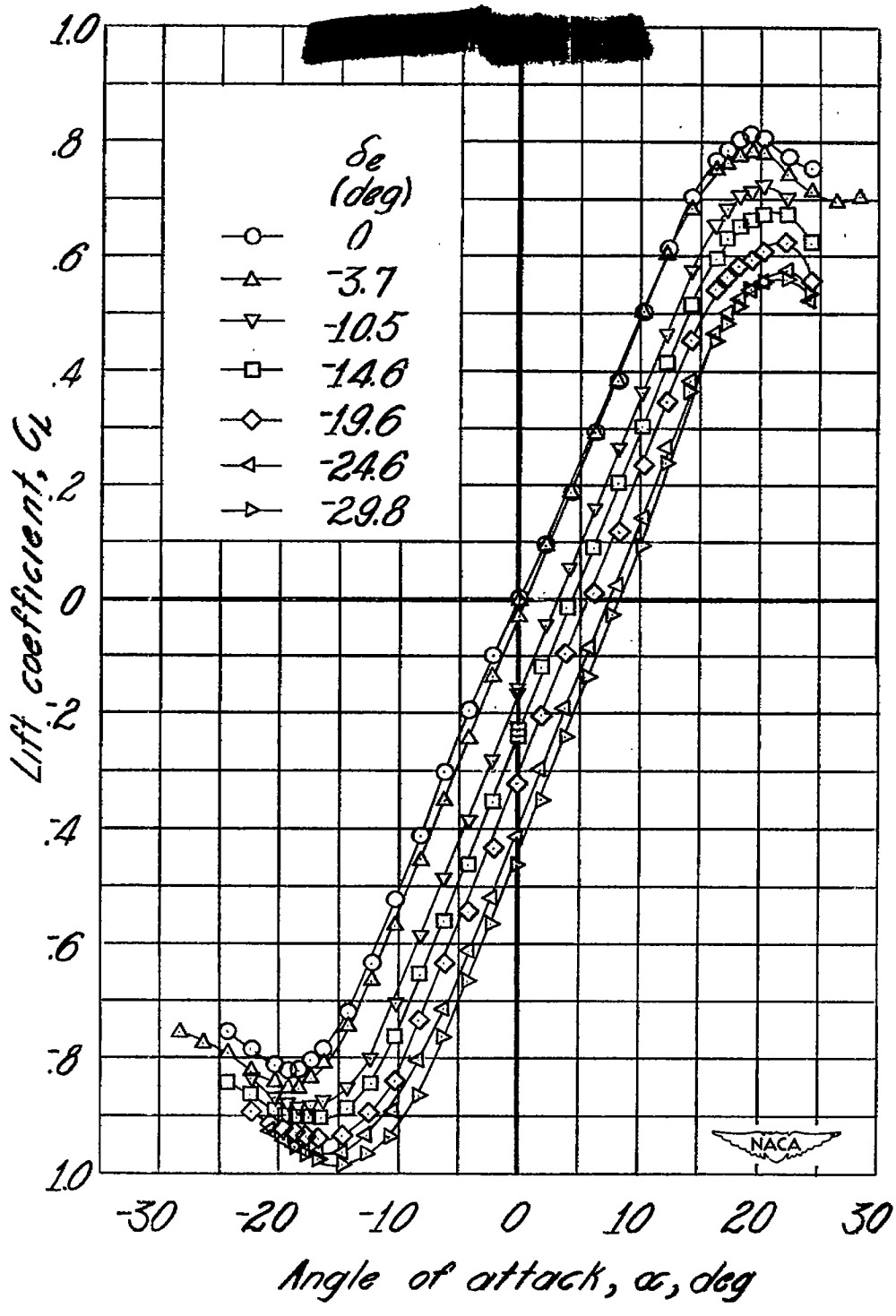

Figure 12.- Aerodynamic characteristics of the 45° sweptback horizontal-tail model equipped [redacted] faired horn. M = 0.70.

[redacted]

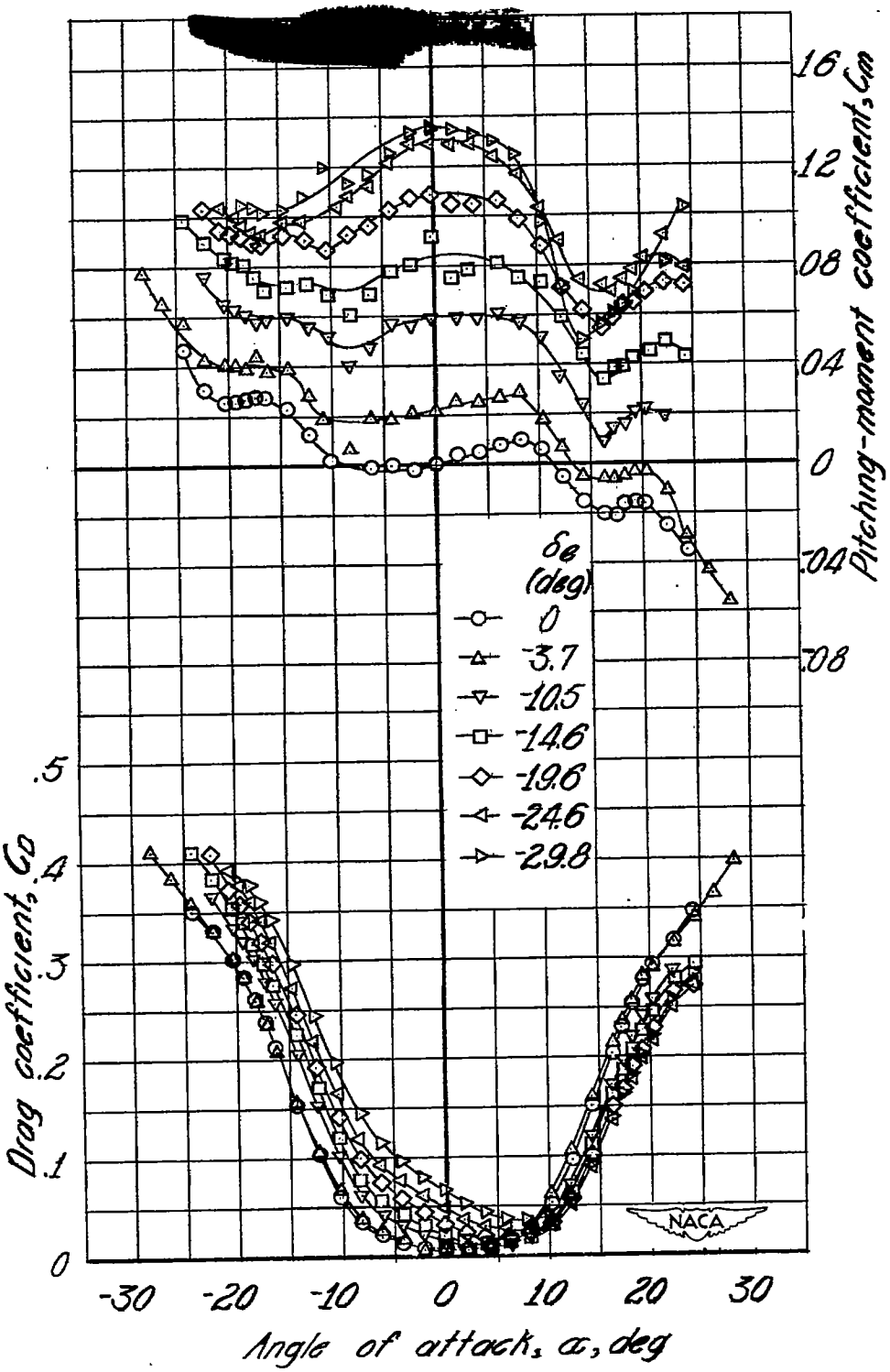

[redacted]ntinued.

[redacted]

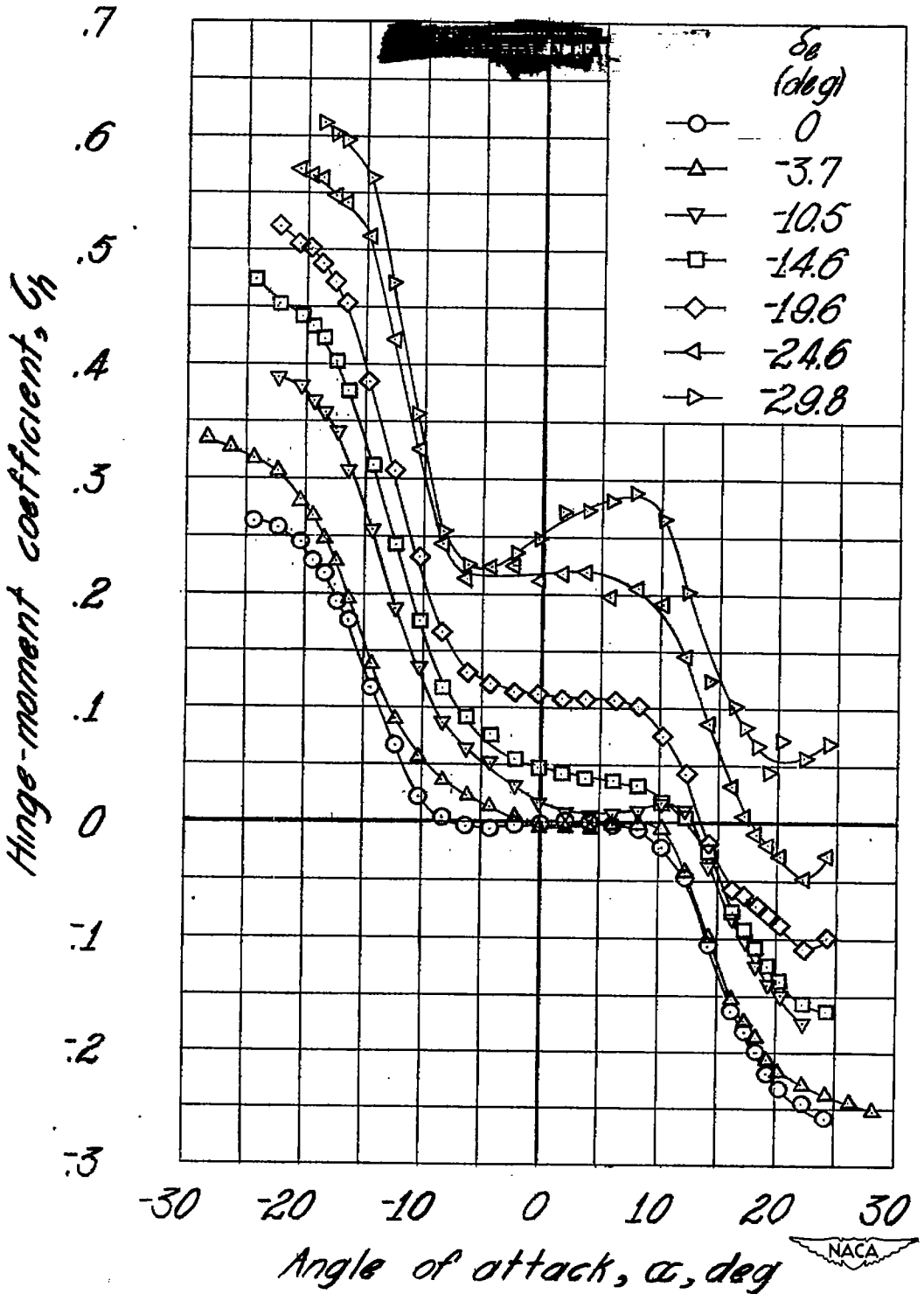

Figure 12.- Concluded.

[redacted]

[redacted]

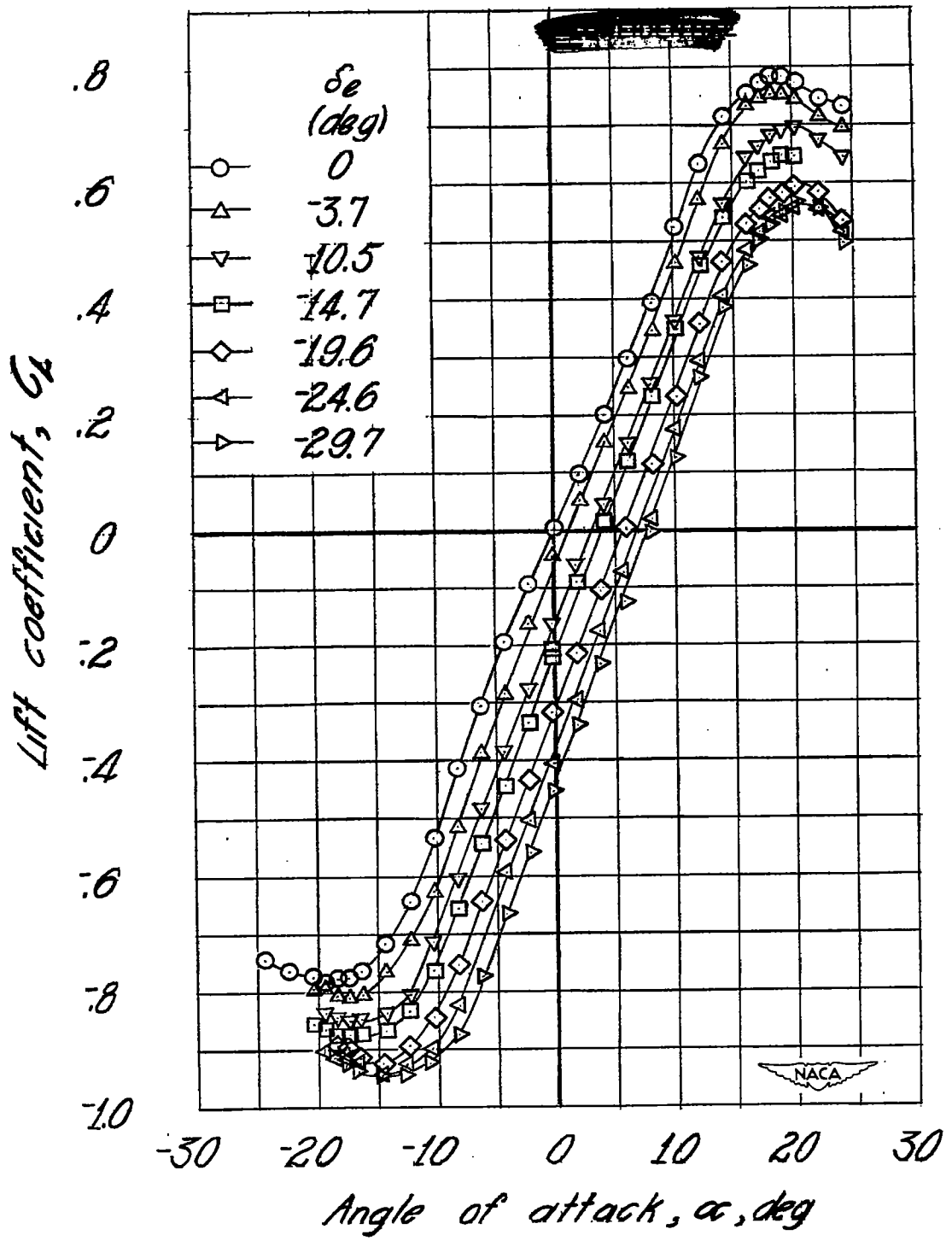

Figure 13.- Aerodynamic characteristics of the 45° sweptback horizontal-tail model equipped with the faired horn. M = 0.75.

[redacted]

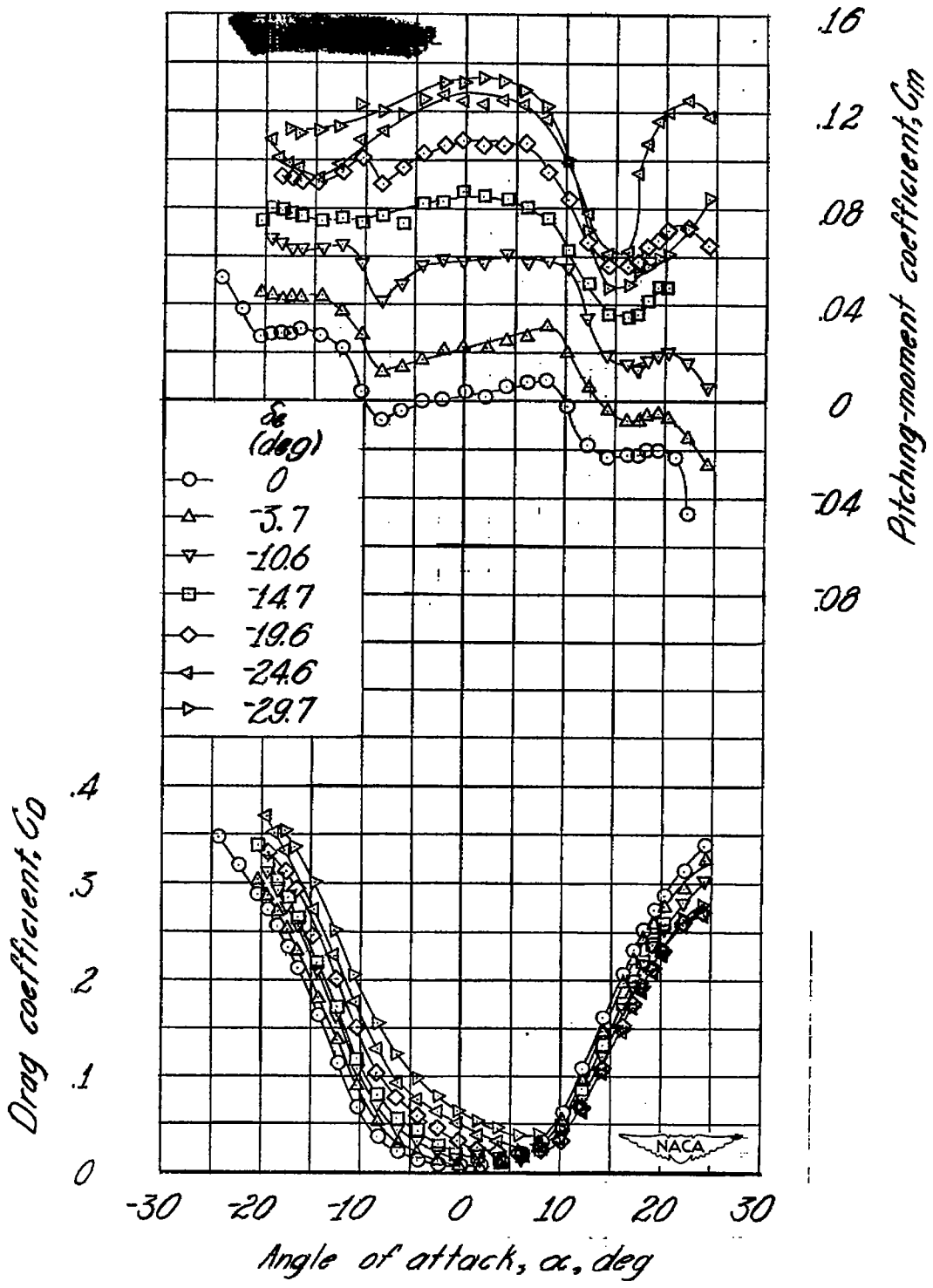

Figure 13.- Continued.

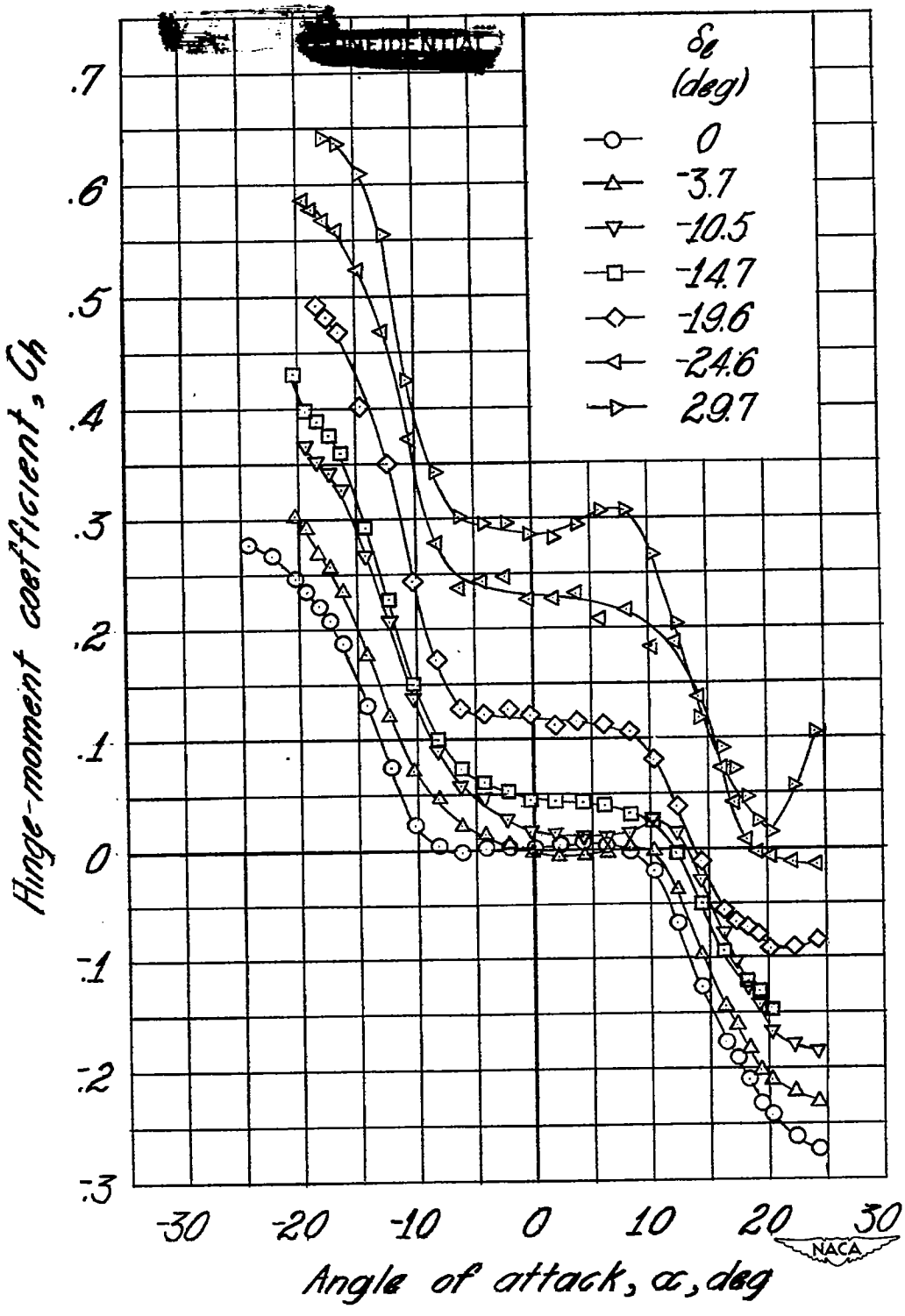

Figure 13.- Concluded.

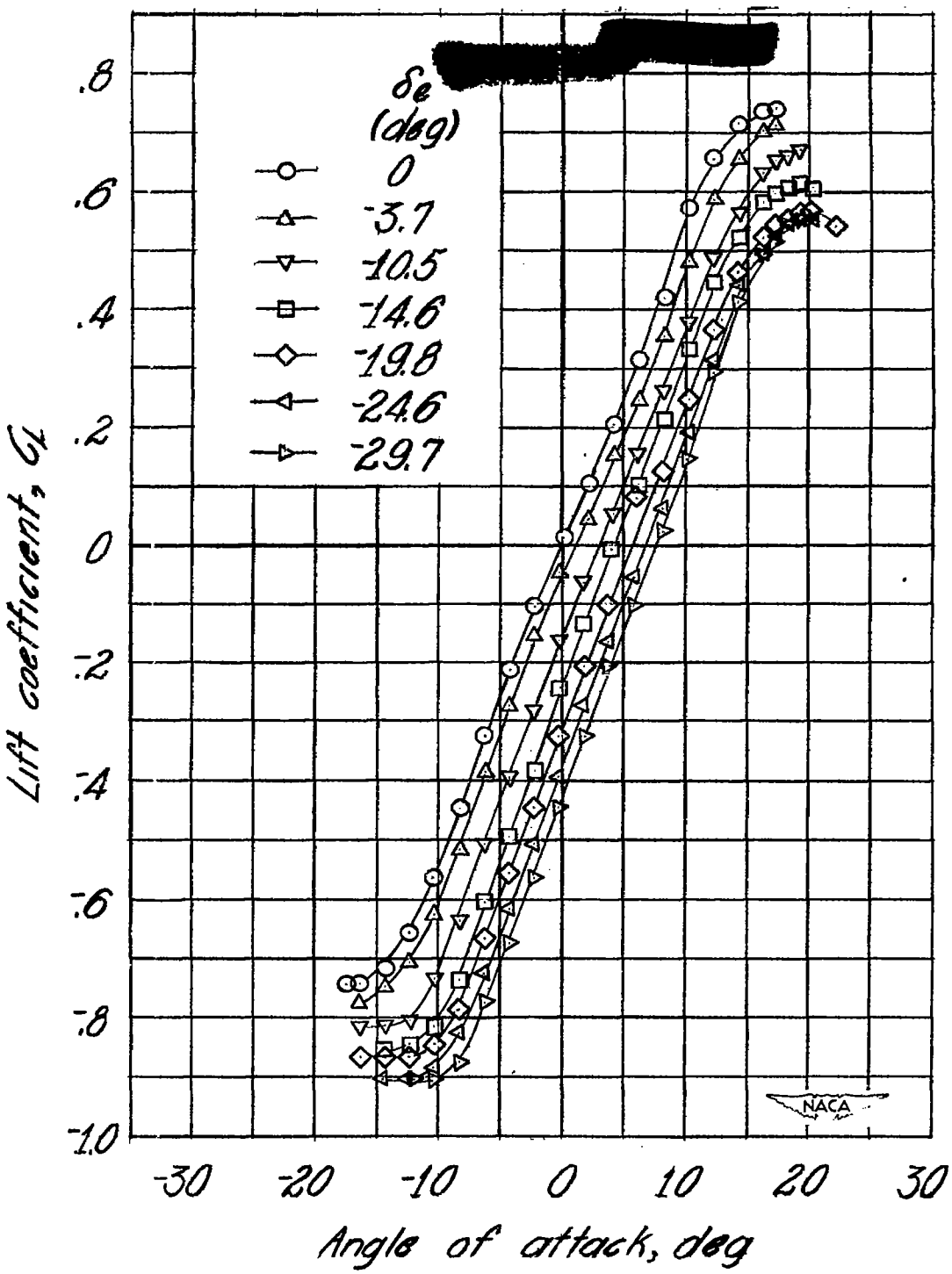

Figure 14.- Aerodynamic characteristics of the 45° sweptback horizontal-tail model equipped with the faired horn. M = 0.80.

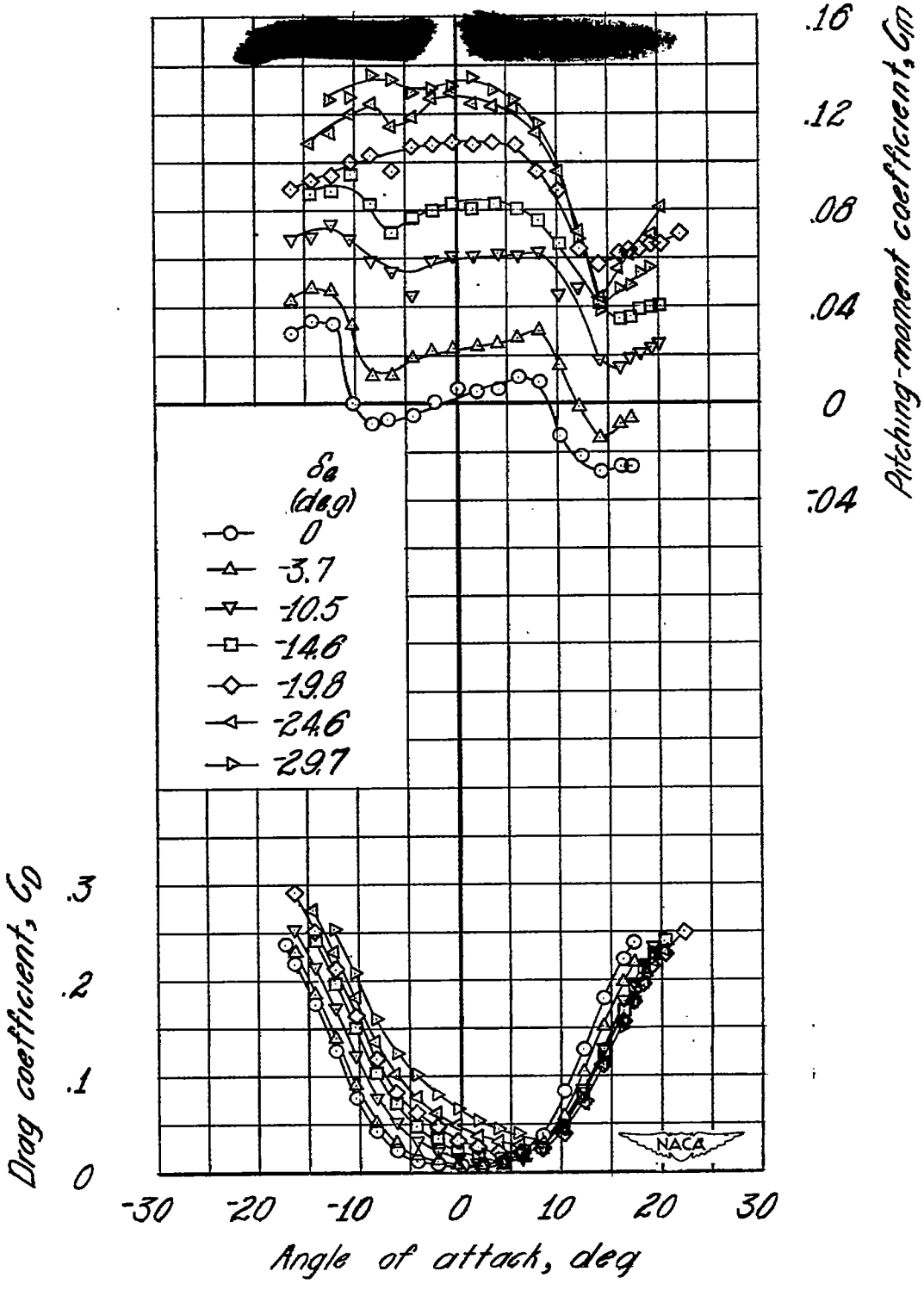

Figure 14.- Continued.

[redacted]

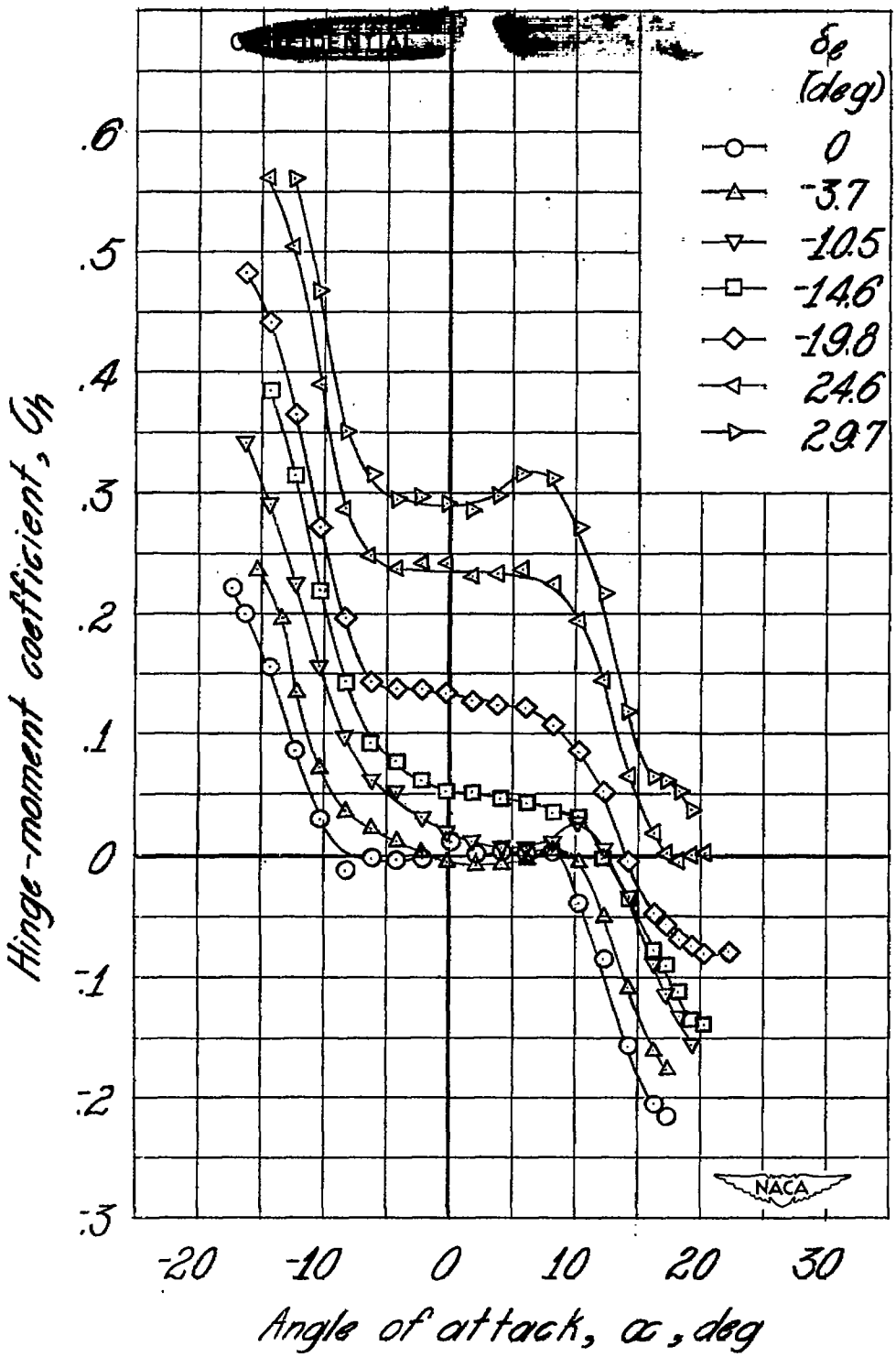

Figure 14.- Concluded.

[redacted]NFIDENTIAL

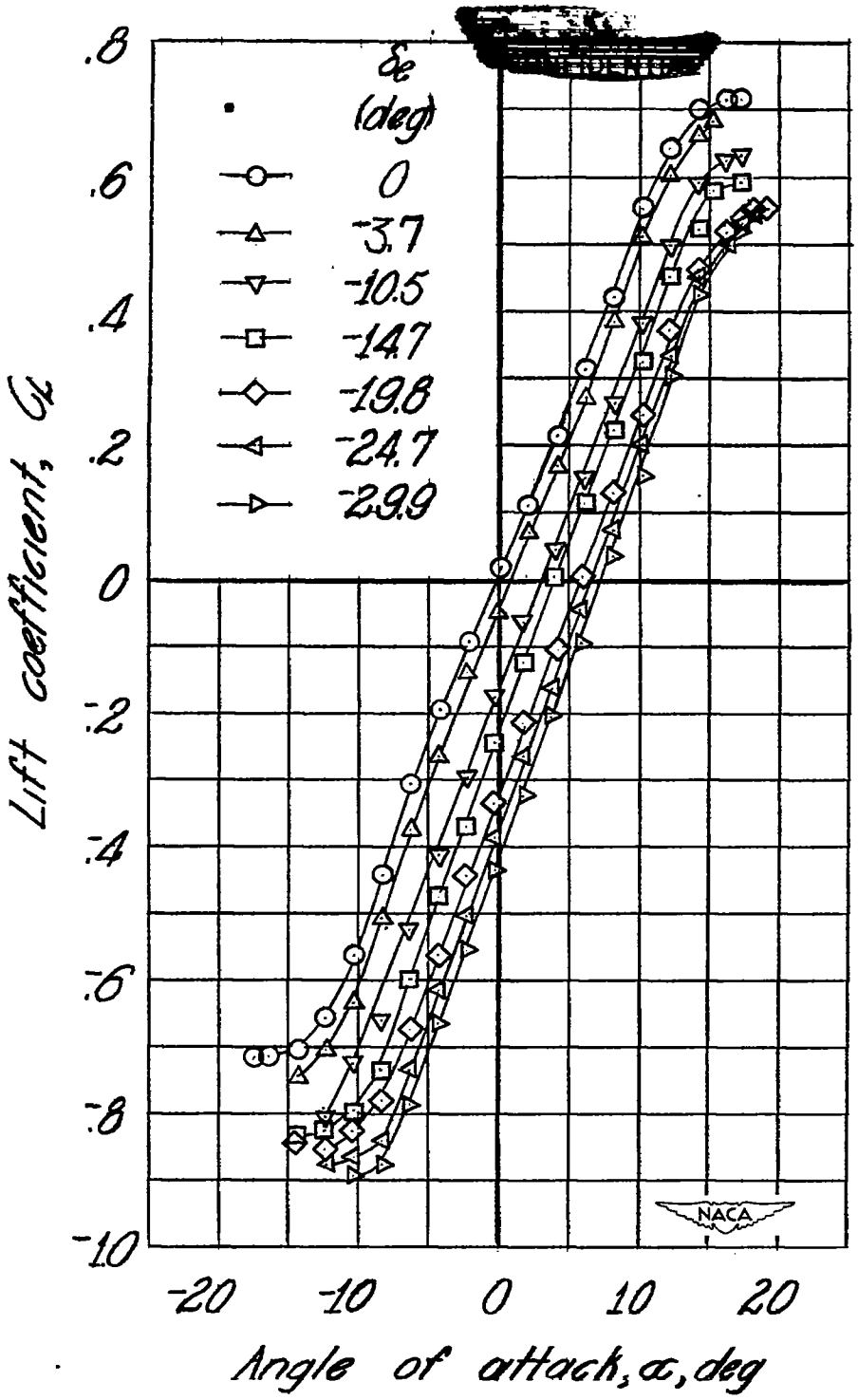

Figure 15.- Aerodynamic characteristics of the 45° sweptback horizontal-tail model equipped with the faired horn. M = 0.82.

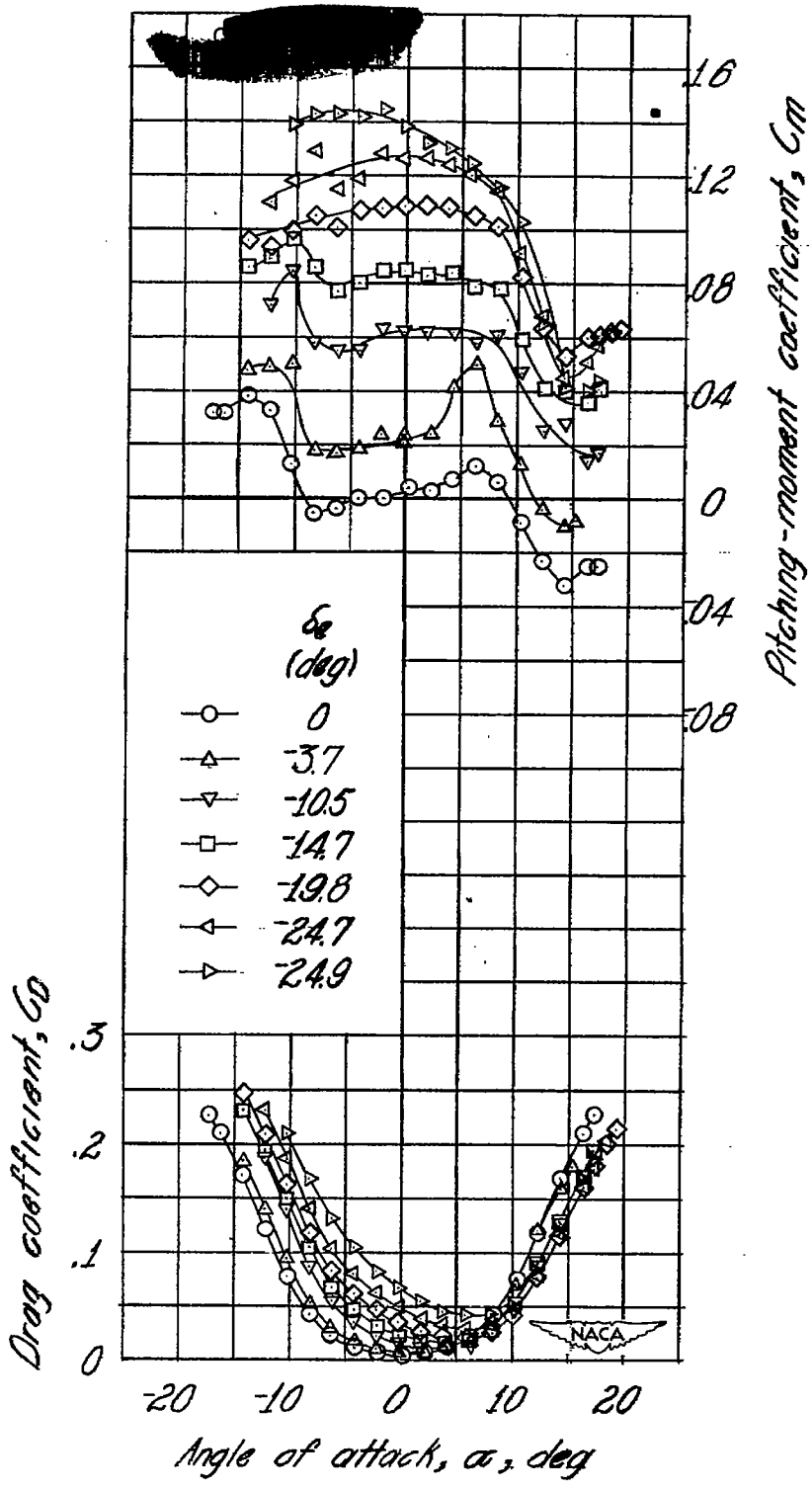

Figure 15.- Continued.

CO[redacted]

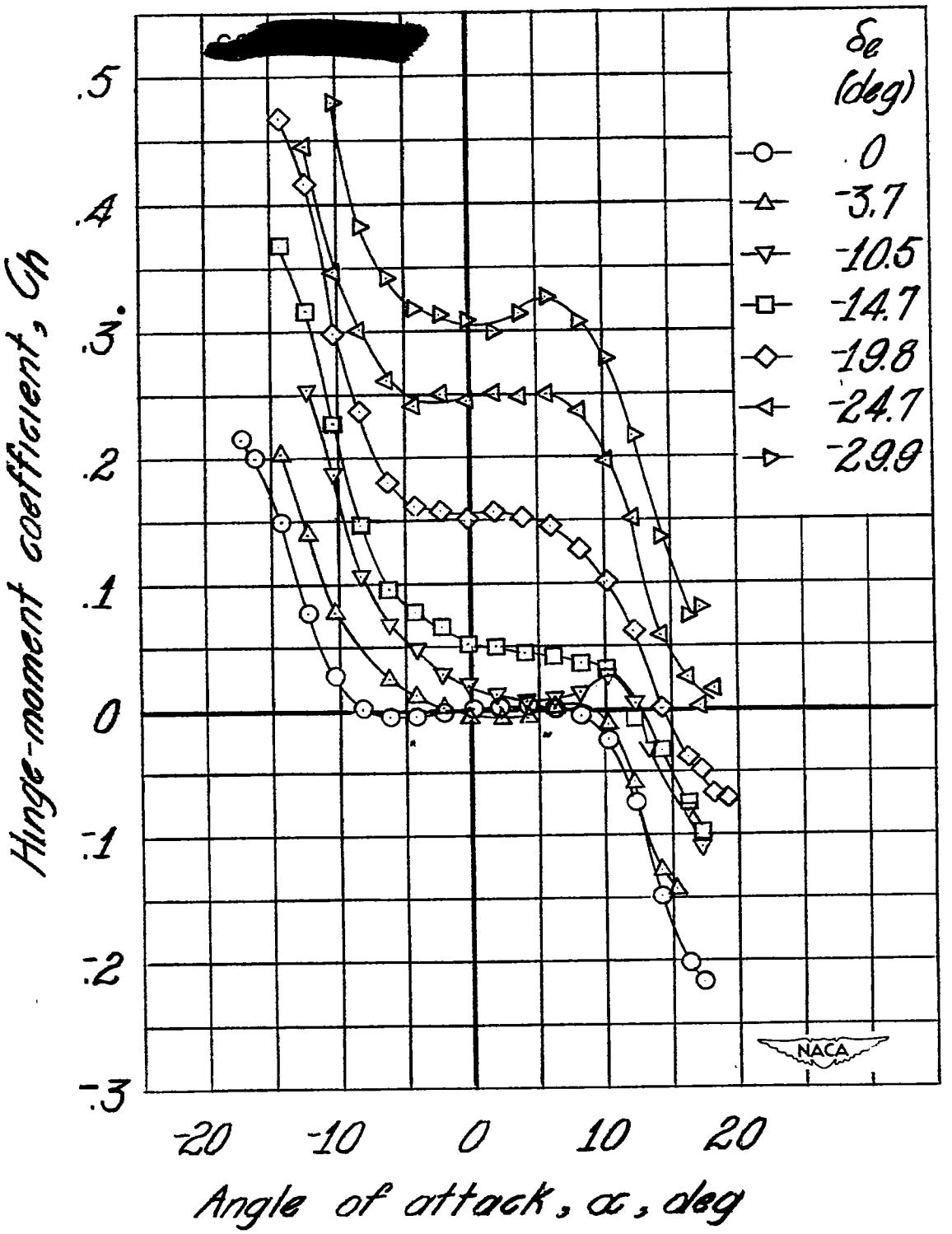

Figu[redacted]cluded.

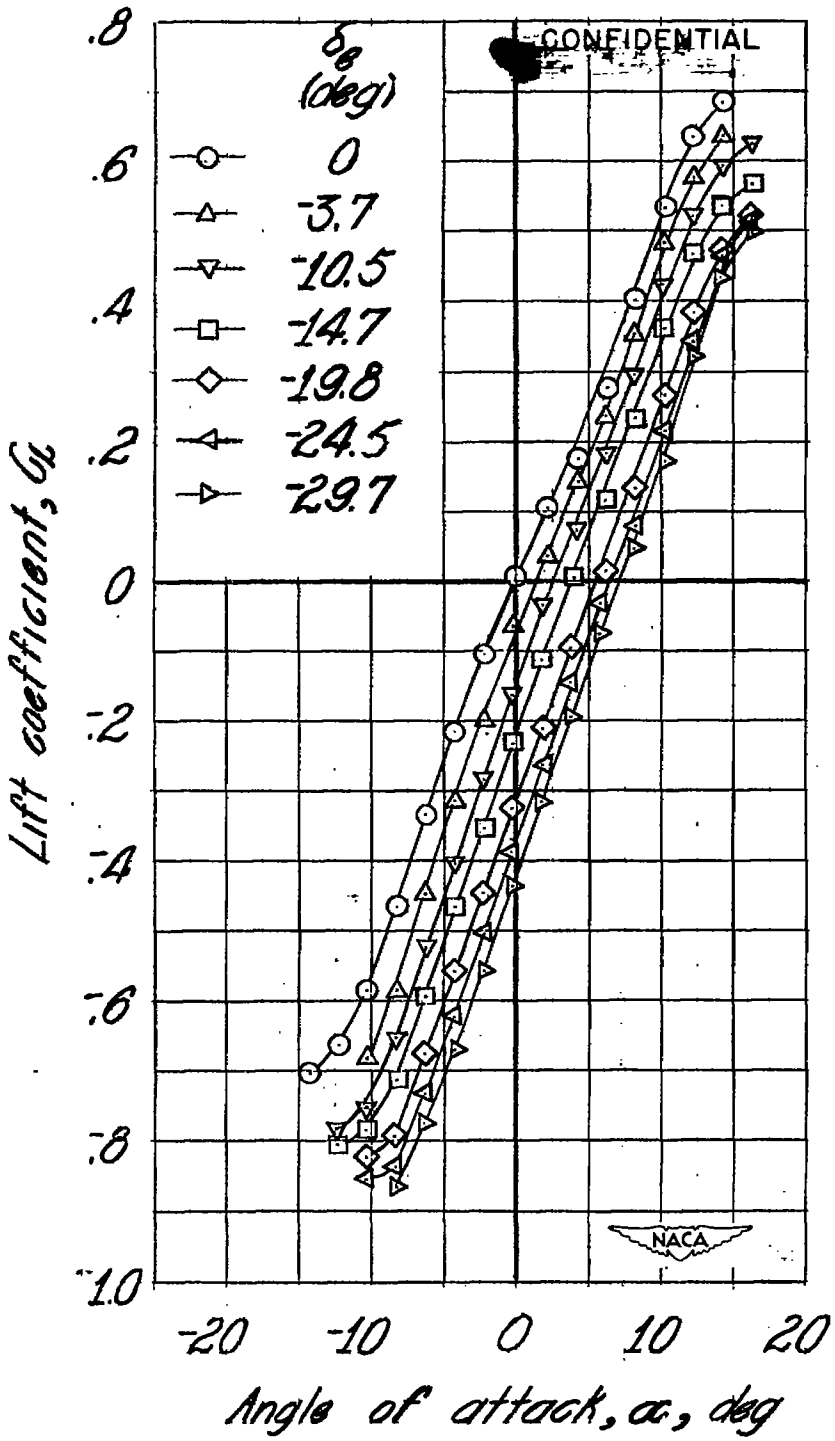

Figure 16.- Aerodynamic characteristics of the 45° sweptback horizontal-tail model equipped with the faired horn. M = 0.84.

[redacted]

[redacted]

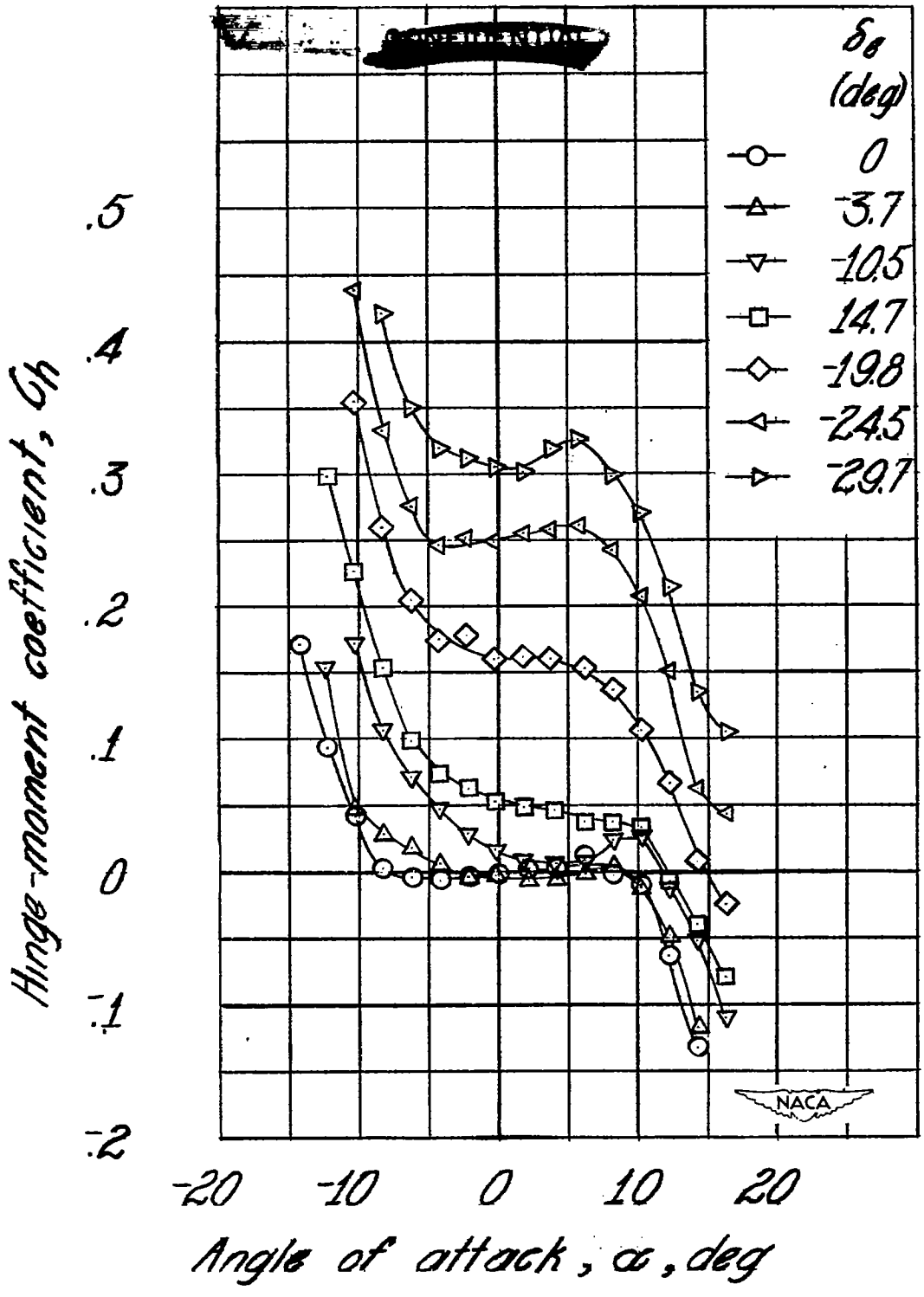

Figure 16.—Concluded.

[redacted]

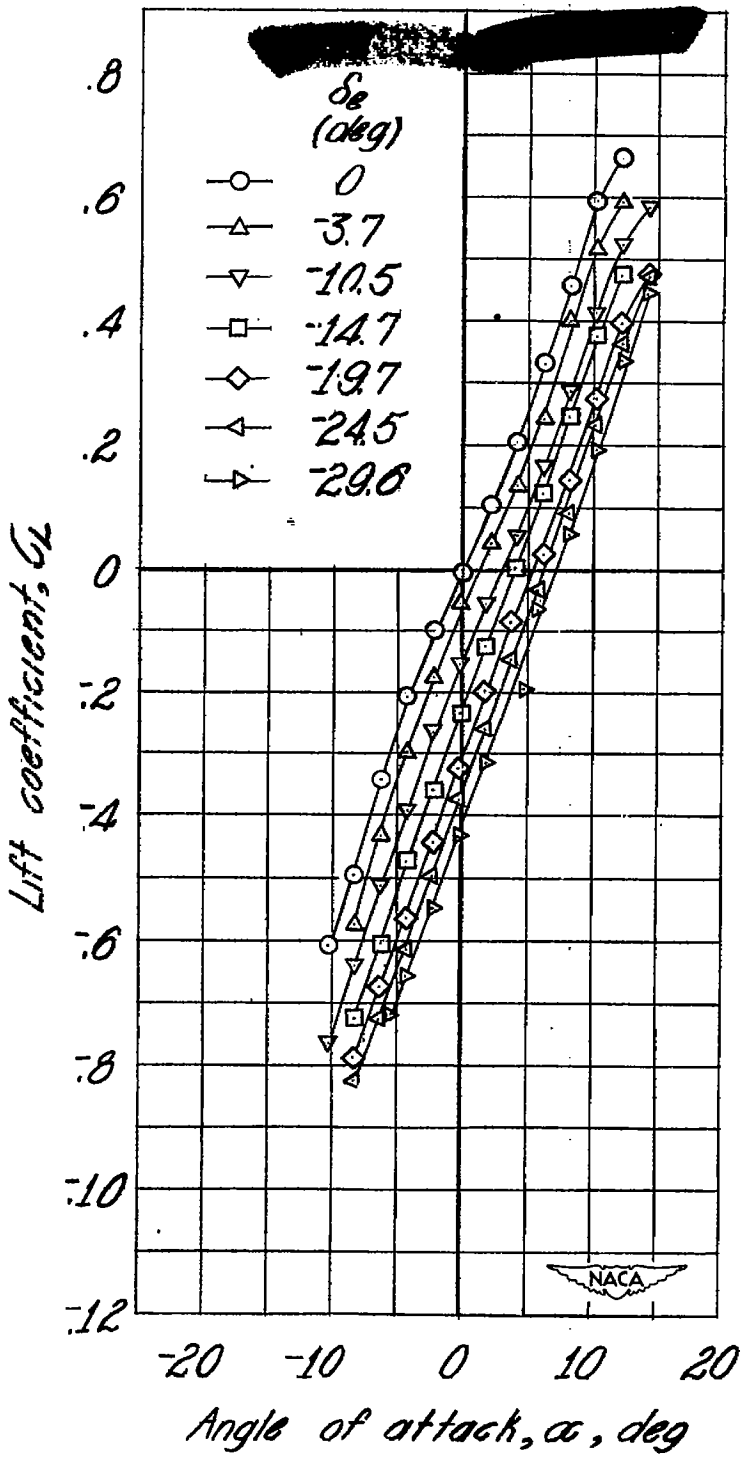

Figure 17.- Aerodynamic characteristics of the 45° sweptback horizontal-tail model equipped with the faired horn. M = 0.86.

[redacted]

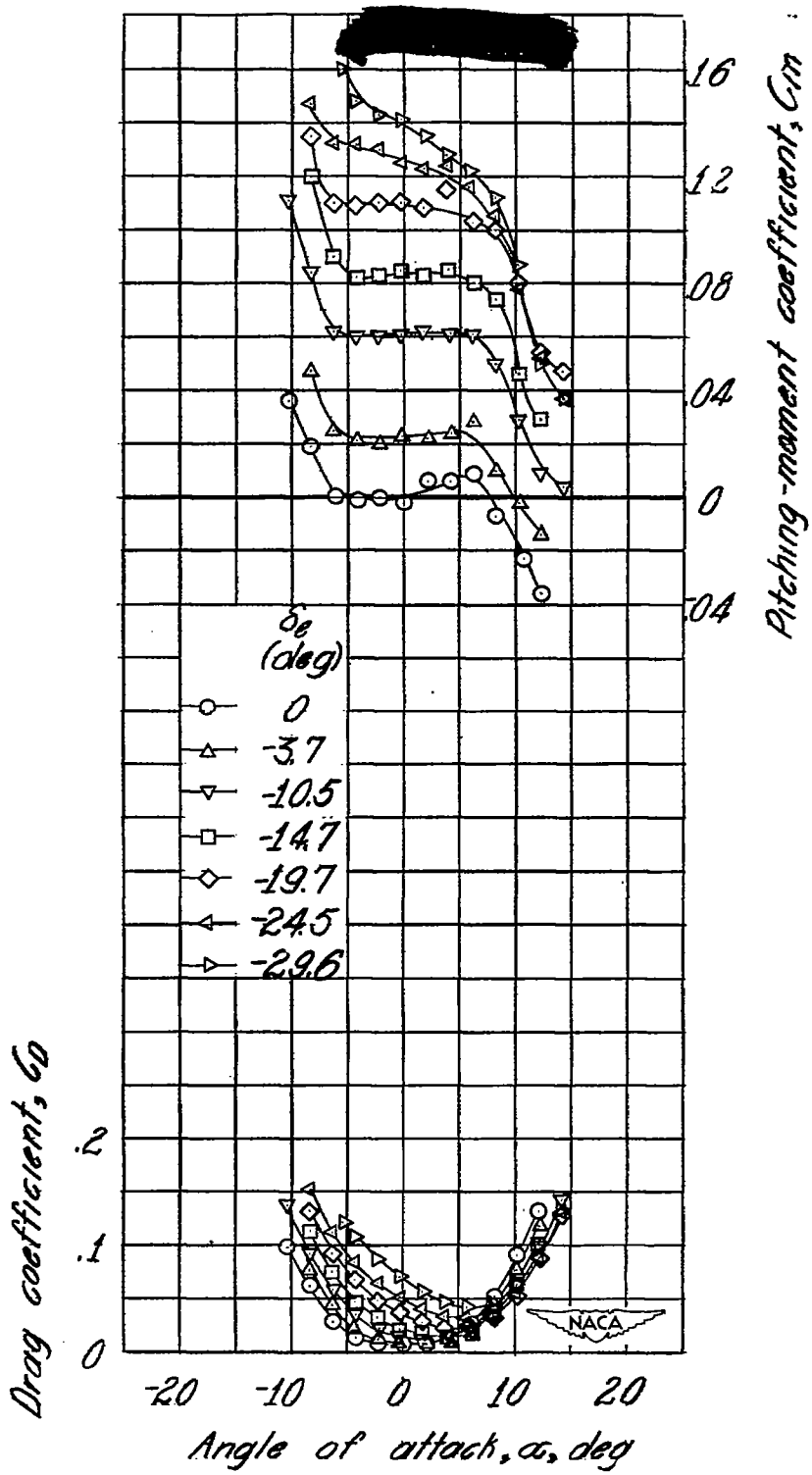

Figure 17.- Continued.

[redacted]

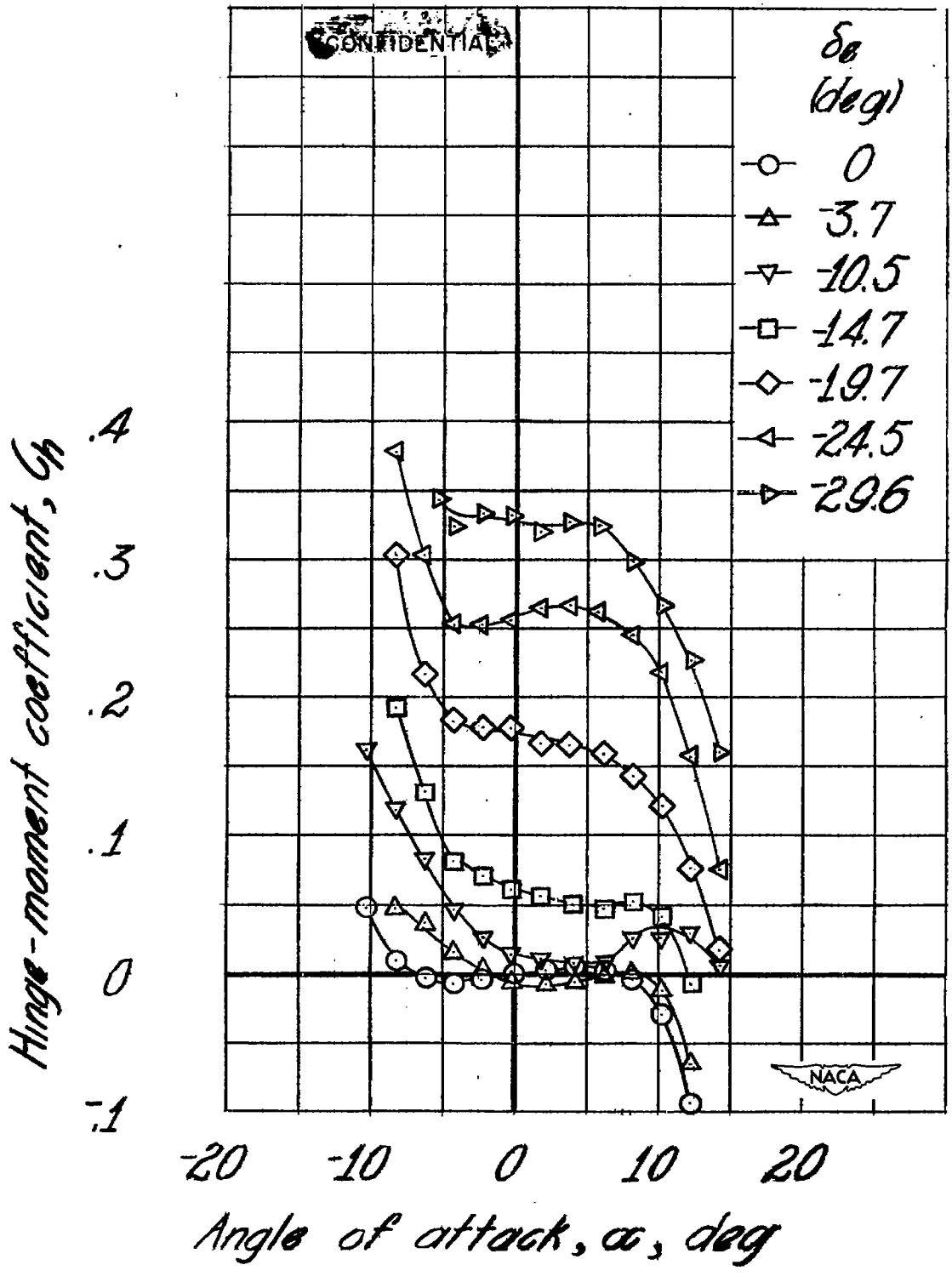

Figure 17.- Concluded.

[redacted]

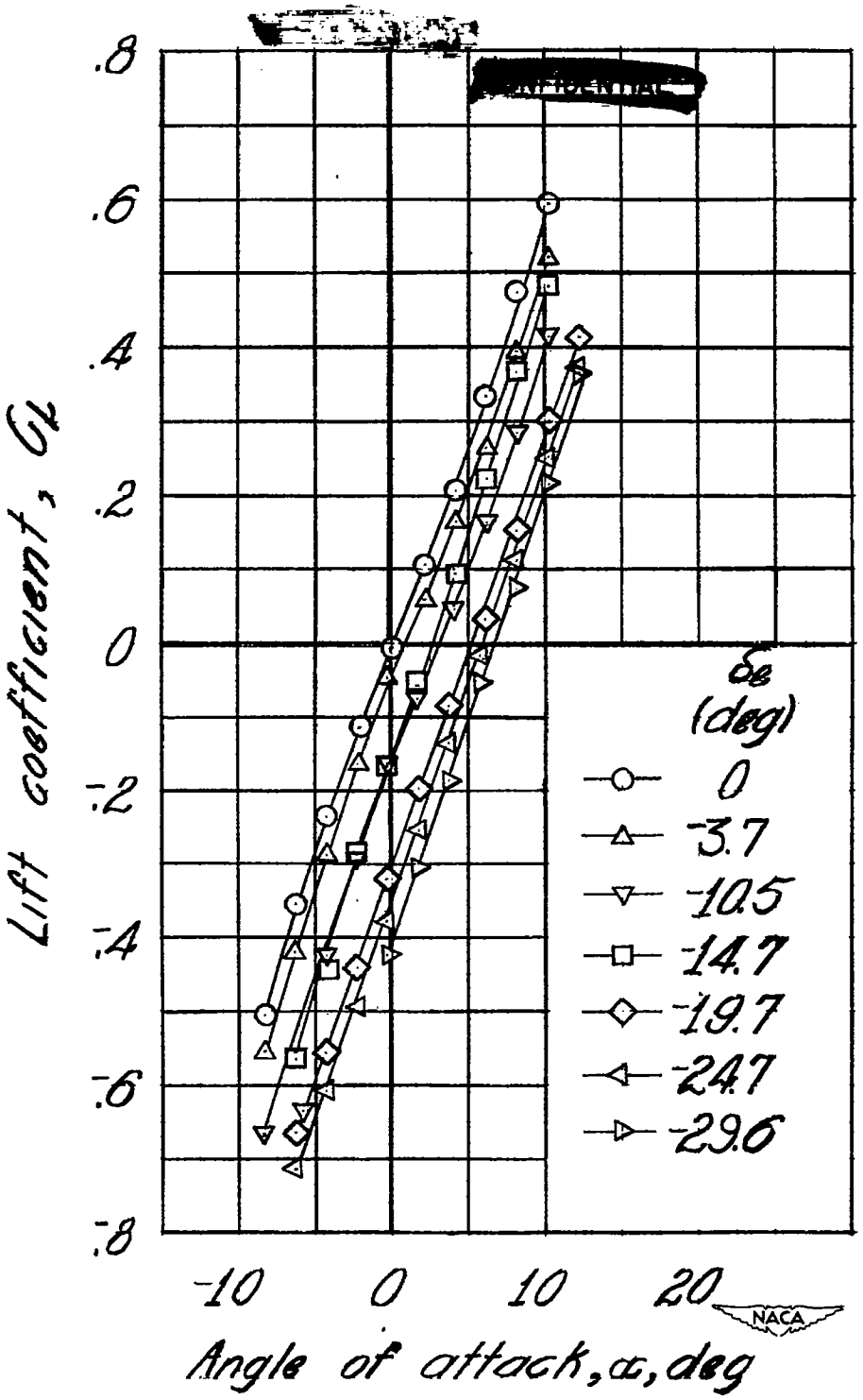

Figure 18.- Aerodynamic characteristics of the 45° sweptback horizontal-tail model equipped with the faired horn. M = 0.89.

[redacted]

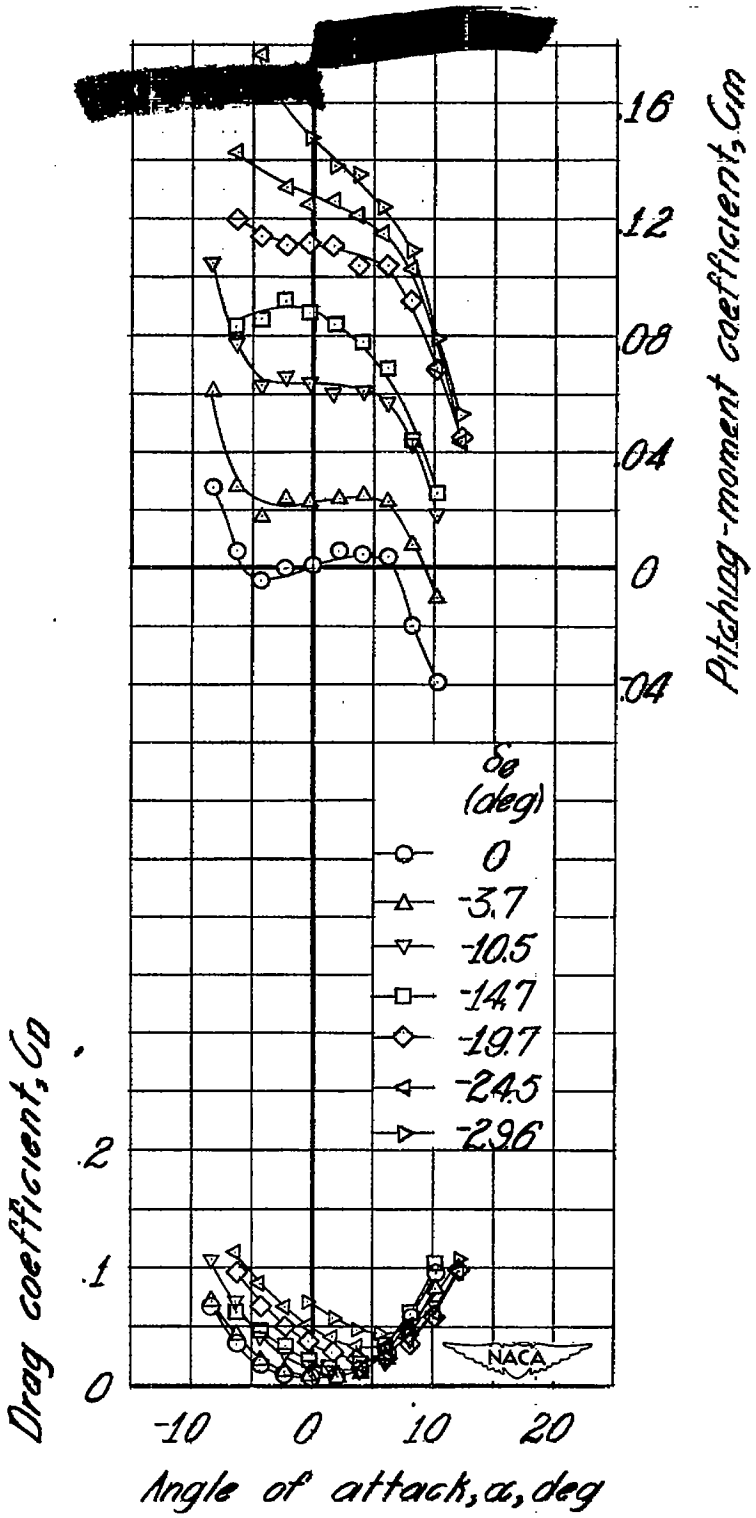

Figure [redacted] Continued.
CON[redacted]

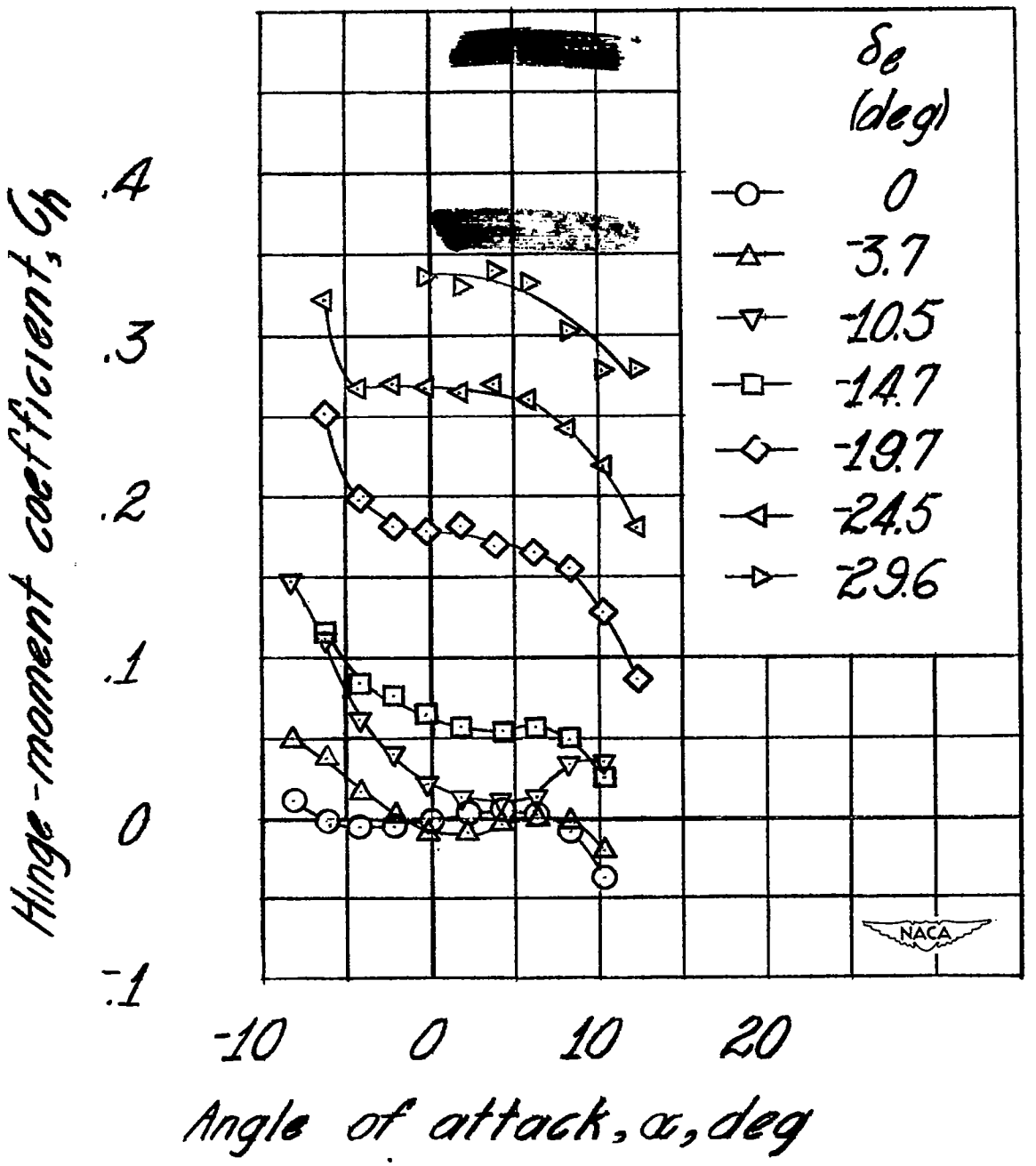

Figure 18.- Concluded.

[redacted]

[redacted]

[redacted]

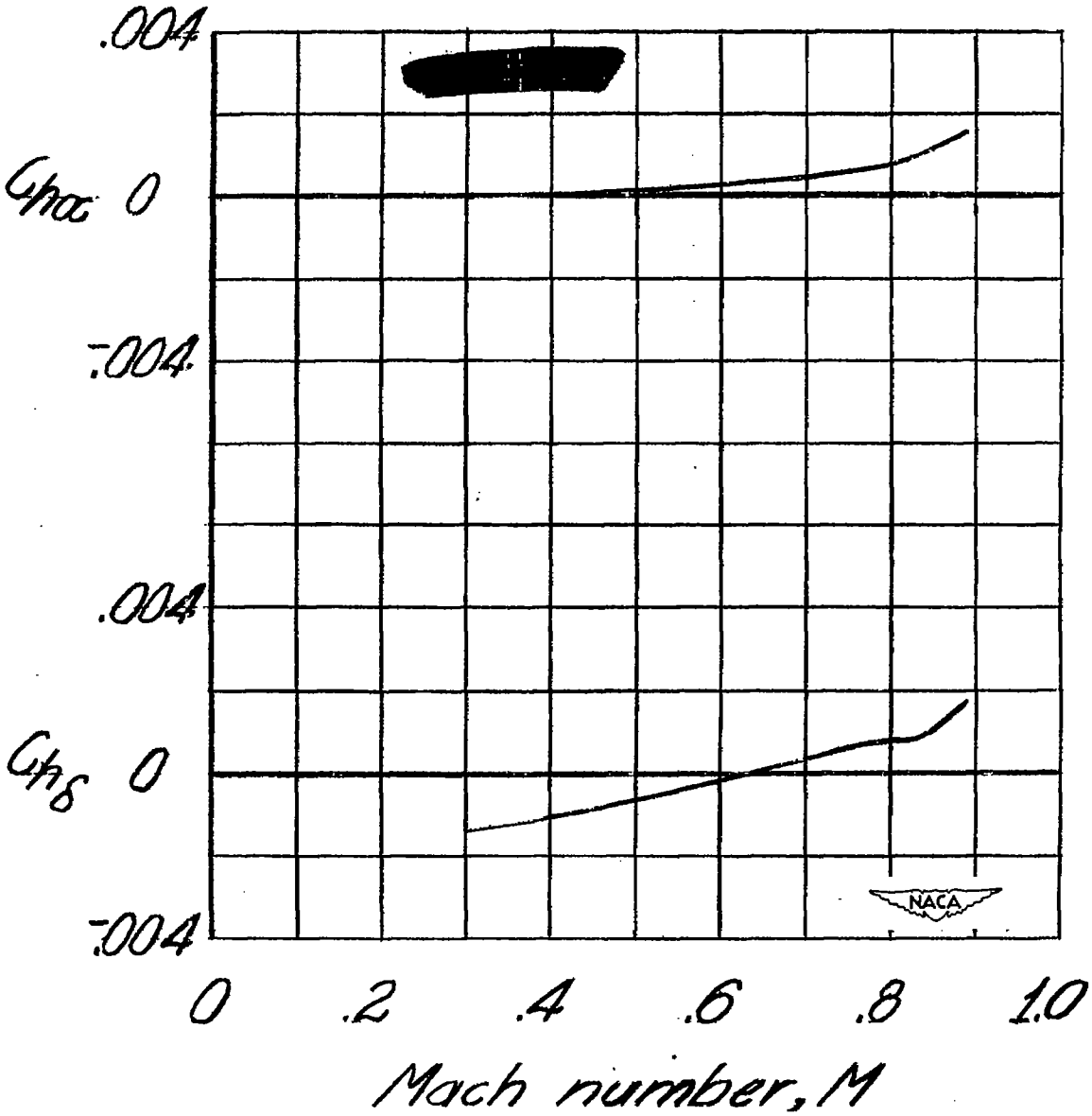

[redacted]

Figure 19.- Effect of Mach number on the hinge-moment parameters. Faired horn.

[redacted]

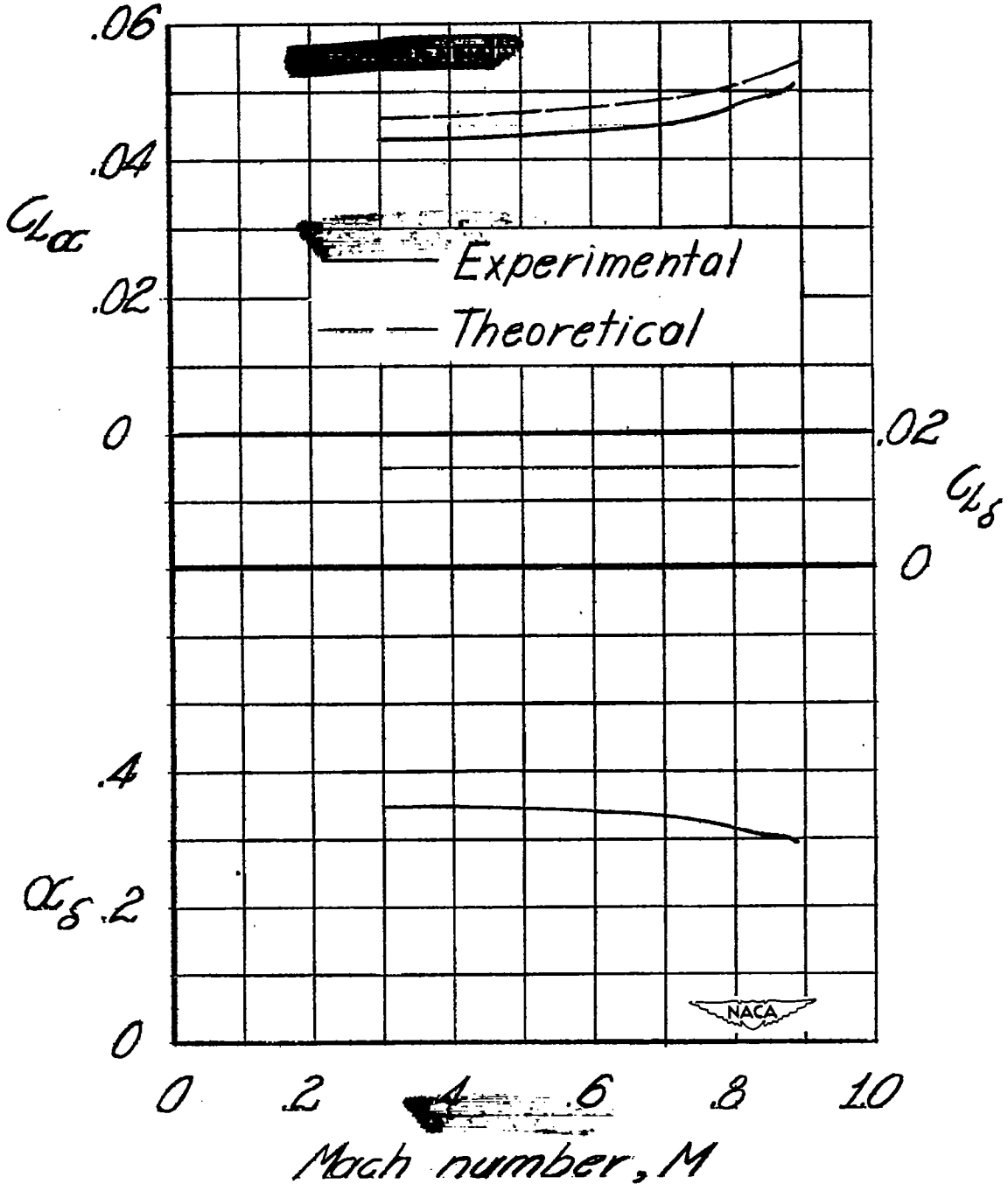

Figure 20.- Effect of Mach [redacted] lift parameters. Faired horn.

[redacted]

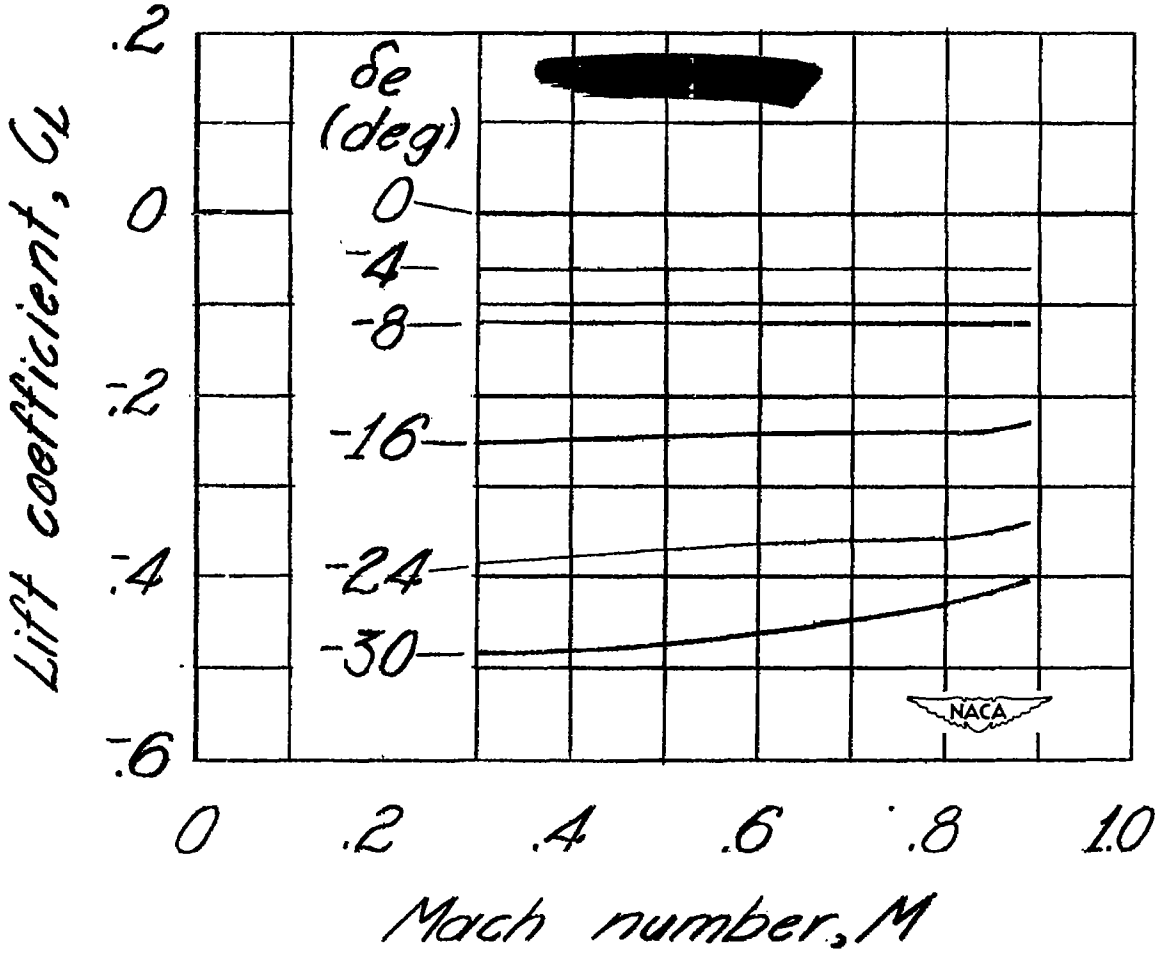

Figure 21.- Effect of elevator deflection on the variation of lift coefficient with Mach number. Faired horn, $\alpha = 0^{\circ}$.

[redacted]

[redacted]

[redacted]

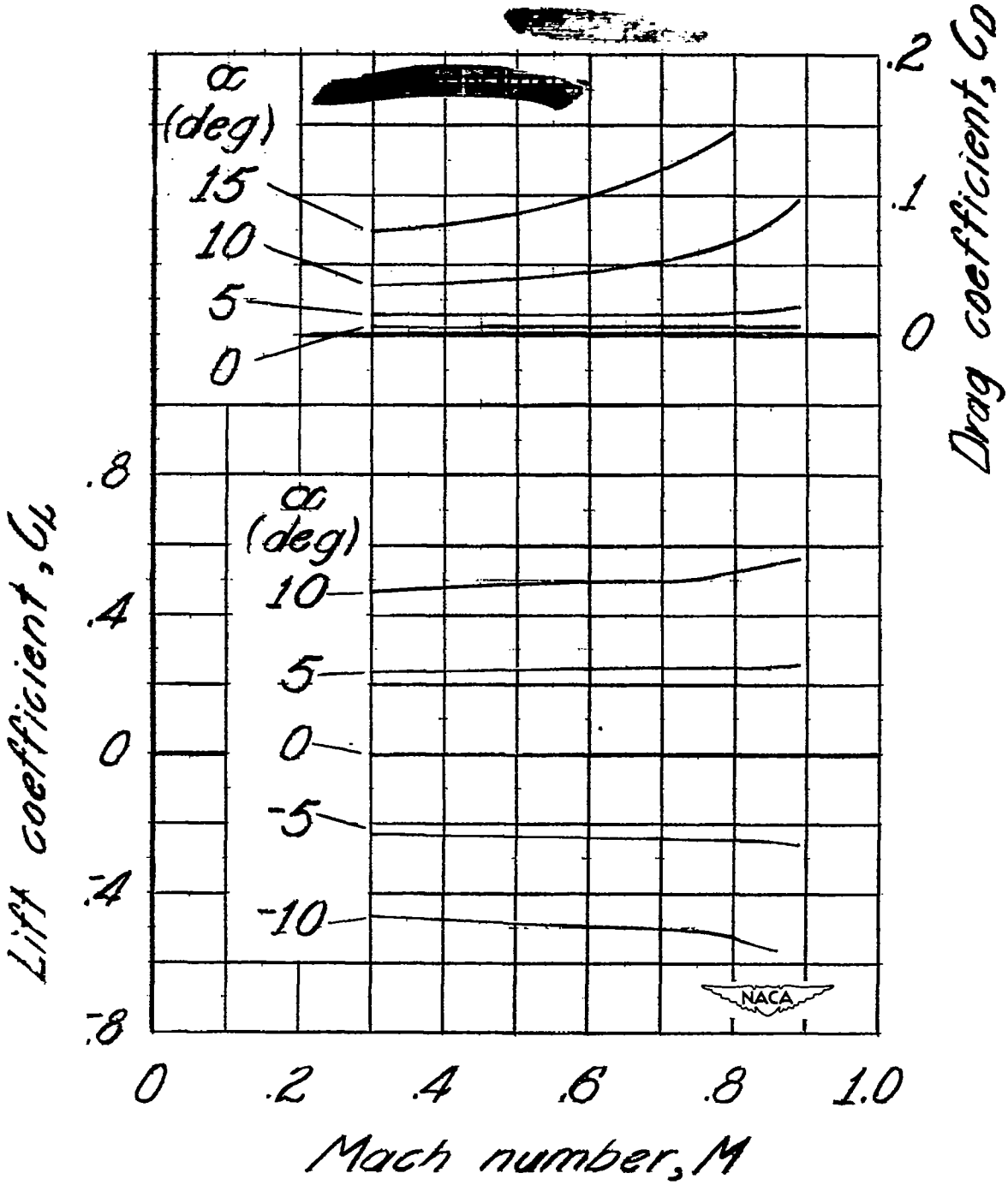

Figure 22.- Variation of lift and drag coefficients with Mach number. Faired horn, $\delta_e = 0^\circ$.

[redacted]

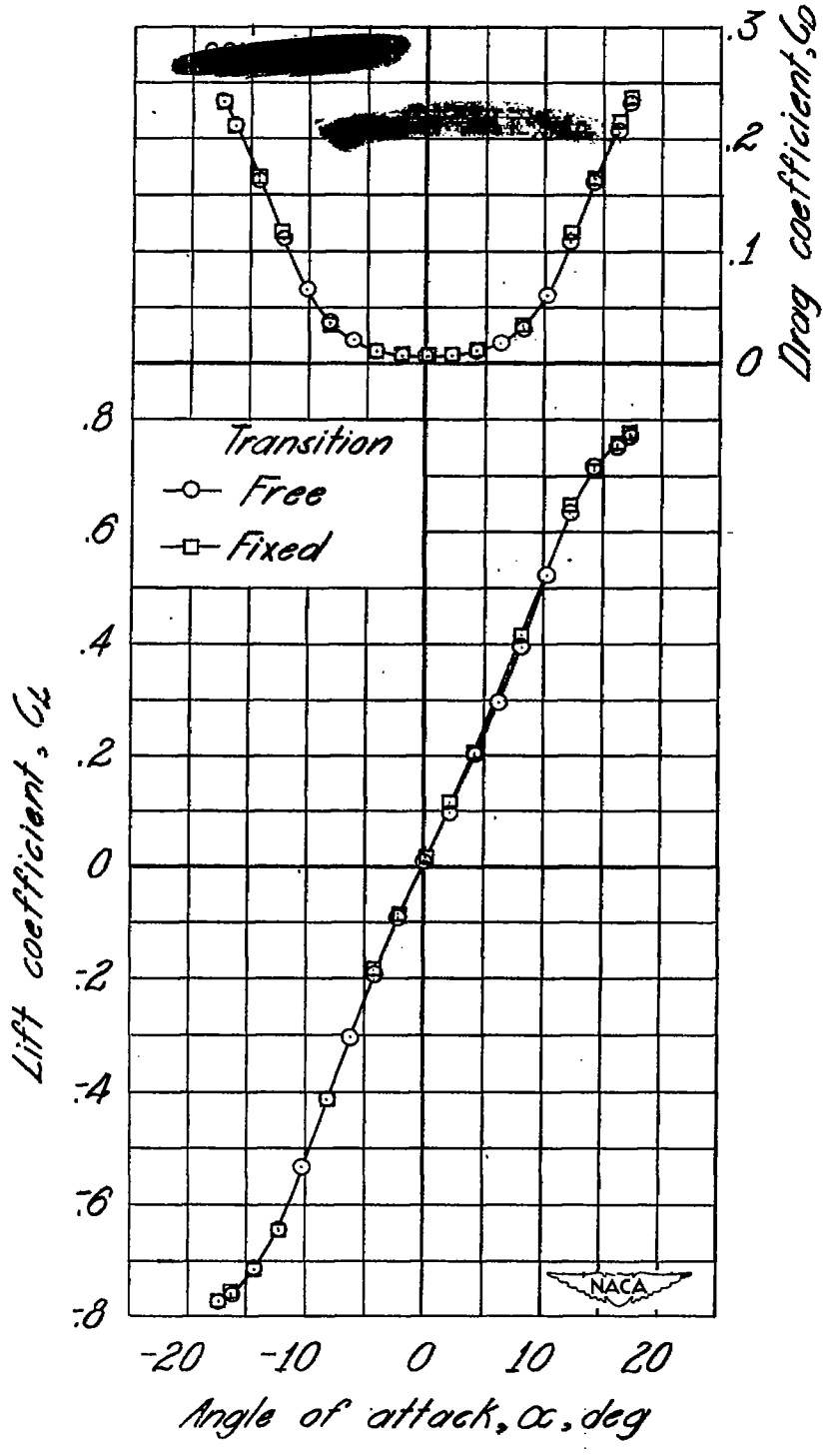

Figure 23.- Effect of fixing transition on the aerodynamic characteristics of the 45° sweptback horizontal-tail model. Faired horn, M = 0.75. [redacted]

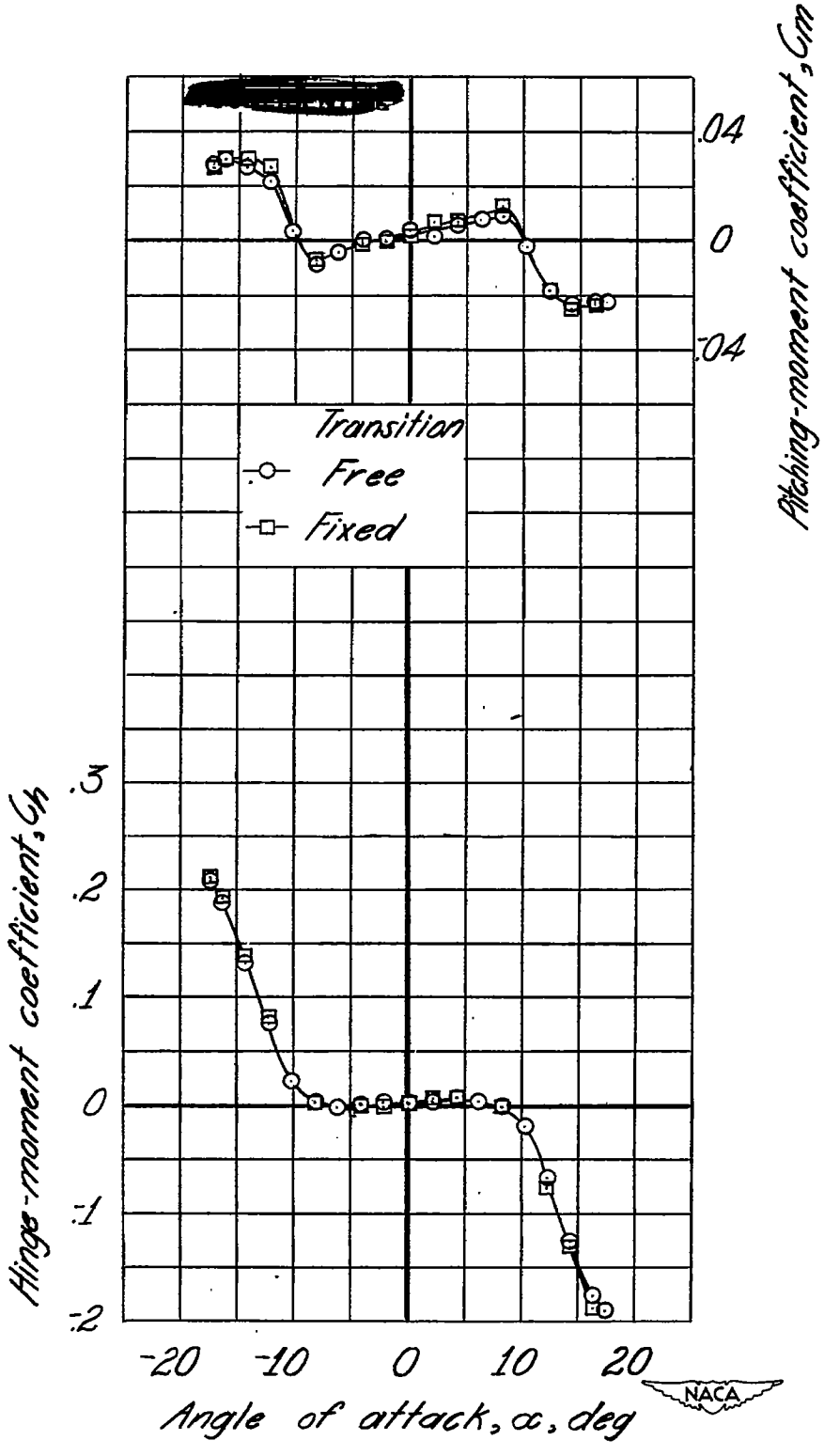

Figure 23.- Concluded.